Comparison of Satellite and Ground-Based NO_2 Measurements in the Mid-Atlantic Region during the 2018 OWLETS-2 Campaign

Alex D. Kaltenbaugh

A scholarly paper in partial fulfillment of the requirements for the degree of

Master of Science

May 2019

Department of Atmospheric and Oceanic Science, University of Maryland
College Park, Maryland

Research Advisor: Dr. Anne Thompson

Table of Contents

Abstract

Nitrogen dioxide (NO_2) is a common air pollutant that is toxic to human respiratory and cardiovascular health. Previous studies have demonstrated the ability of satellites (Aura OMI) and ground-based spectrophotometers (PSI) to detect NO_2 pollution in urban areas around the world. However, the ability to validate the instruments in coastal regions has remained difficult due to OMI's coarse spatial resolution as well as the inhomogeneity of the surfaces. Data from the Sentinel-5 Precursor's Tropospheric Monitoring Instrument (TROPOMI) became available in June 2018, and the instrument's spatial resolution is nine times higher than that of OMI. This study compares column NO_2 measurements from PSI with those from OMI and TROPOMI during the 2018 OWLETS-2 campaign. Comparisons are performed at two sites: NASA Goddard Space Flight Center (GSFC) and the University of Maryland, Baltimore County (UMBC). TROPOMI's higher resolution allowed for mean satellite-PSI agreement to fall within 10% at the less-polluted GSFC site and within 20% at the more-polluted UMBC site. In addition, statistically significant correlations between satellite and ground-based NO_2 measurements were found at both sites. Case studies conducted on 29 June and 30 June illustrate these results and show that as vertical mixing increases the homogeneity of the surface layer throughout the day, satellite-PSI comparisons improve by a factor of two.

Acknowledgements

I would like to thank Dr. Anne Thompson for all of her guidance and support as my advisor while conducting my graduate research. In addition, I would like to thank Dr. Debra Kollonige, Dr. Ryan Stauffer, and Dr. Russell Dickerson for all of their guidance and support with this project. Support for this project came from the National Aeronautics and Space Administration (NASA) and the U.S. Department of the Interior, Bureau of Ocean Energy Management (BOEM) through Interagency Agreement M17PG00026 with NASA (B. Duncan, PI).

List of Tables

Table: **Page:**

List of Figures

Figure: **Page:**

Supplementary Figures: **Page:**

Chapter 1. Introduction

Nitrogen dioxide (NO_2) is a widely occurring air pollutant that is toxic to human respiratory and cardiovascular health (Yang et al., 2009; Gurji et al., 2010; Lamsal et al., 2015; Goldberg et al., 2017). In addition to its adverse health impacts, NO_2 is of interest to scientists because of its unique absorption features within the UV-visible region of the electromagnetic spectrum (Knepp et al., 2015; Lamsal et al., 2017; Goldberg et al., 2017). Thus, satellite instruments like NASA's Aura Ozone Monitoring Instrument (OMI) use measurements of solar backscatter to estimate total column NO_2 (Bucsela et al., 2013; Knepp et al., 2015; Martins et al., 2016; Lamsal et al., 2017; Goldberg et al., 2017). Over the past decade, studies like Lamsal et al. (2015) and Duncan et al. (2016) have shown that OMI is able to monitor NO_2 over urban environments and rural biomass burning regions around the world.

In addition to satellite instruments, NASA's ground-based Pandora spectrophotometer instruments (PSI) can measure total column NO_2. PSI measures direct solar radiation and uses the absorption spectra to estimate total column NO_2, similar to OMI. However, PSI can provide continuous NO_2 measurements throughout the day with a temporal resolution on the order of minutes. This allows for an analysis of the diurnal variability of NO_2 pollution, which is not possible with 1-2 daily satellite overpasses (Tzortziou et al., 2018; Kollonige et al., 2018). Since nitrogen oxides ($NOx = NO + NO_2$) are often emitted from the surface through fossil fuel combustion, ground-based measurements from PSI can provide useful approximations of surface and planetary boundary layer (PBL) NO_2 pollution (Herman et al., 2009; Tzortziou et al., 2012; Tzortziou et al., 2015; Knepp et al., 2015).

In order to validate the satellite NO_2 retrievals, previous studies have compared measurements from OMI with those from PSI. Tzortziou et al. (2012) found that OMI-PSI differences for NO_2 ranged from 0.05 Dobson units (DU) to 0.17 DU (~20-50% difference) at 12 sites in the Baltimore/Washington region. In addition, PSI NO_2 retrievals varied by an order of magnitude spatially and temporally, which indicated that PSI was able to resolve localized pollution gradients (Tzortziou et al, 2012). Similarly, Reed et al. (2015) compared OMI and PSI column NO_2 retrievals during the 2011 DISCOVER-AQ campaign in the Baltimore/Washington region. The study found that OMI and PSI agreed within 25% during most coincident observations, but the presence of clouds and/or aerosols degraded the percent differences by nearly a factor of 3, resulting in offsets as high as 65%. Tzortziou et al. (2012) and Reed et al. (2015) both observed that PSI generally registered more total column NO_2 than OMI.

More recently, the Herman at al. (2018), Tzortziou et al. (2018), and Kollonige et al (2018) studies made OMI-PSI NO_2 comparisons in coastal environments. During the 2016 KORUS-AQ campaign in Korea, Herman et al. (2018) found OMI-PSI total column NO_2 differences of 0.12 +/- 0.15 DU in polluted urban areas like Seoul and Busan. This indicated that the satellite and ground-based total column NO_2 measurements differed by roughly a factor of two with PSI typically measuring more total column NO_2 than OMI. Tzortziou et al. (2018) also compared total column NO_2 measurements from OMI and PSI during KORUS-AQ. The OMI-PSI agreement varied considerably among various sites, and PSI measured 10-50% more total column NO_2 than OMI. Kollonige et al. (2018) found overall OMI-PSI agreement of ~20% at various terrestrial and marine sites that were subject to periodic regional pollution. As was the case in Herman et al. (2018) and Tzortziou et al. (2018), OMI generally measured less total column NO_2 than PSI. Herman et al. (2019) found that OMI measured on average 25-30% less

total column NO_2 than PSI at numerous sites around the world. These results indicate that OMI has a tendency to underestimate the total column NO_2 in highly polluted environments.

Despite promising results, the validation of satellite and PSI measurements in coastal urban environments remains an ongoing challenge. These environments can have a variety of emission sources (i.e., mobile, shipping, power plants, etc.) as well as complex meteorological phenomena associated with land-water interfaces (Tzortziou et al., 2012; Stauffer et al., 2015; Tzortziou et al., 2015; Sullivan et al., 2018). As mentioned previously, clouds and aerosols can interfere with the satellite and ground-based retrievals and worsen the agreement between the two instruments (Reed et al., 2015). Bay- and sea-breeze circulations can arise in coastal environments due to hydrostatic pressure gradients resulting from differential heating between land and water surfaces (Stauffer et al., 2012; Flynn et al., 2016). These circulations can rapidly transport low-level NO_2 pollution both horizontally and vertically (Flynn et al., 2016; Sullivan et al., 2018). In addition, the distribution of NO_2 pollution in the vertical by turbulent mixing can influence comparisons. Satellites are generally more sensitive to pollution that is located higher up in the atmosphere, which means that NO_2 pollution that is trapped near the surface may go undetected (Lamsal et al., 2017; Goldberg et al., 2017; Kollonige et al., 2018). Thus, vertical mixing can redistribute NO_2 pollution aloft and improve satellite-PSI comparisons.

In addition to meteorology, satellite retrievals can also suffer from inhomogeneities between land and water surfaces that result from differences in surface reflectivity and absorptivity (Tzortziou et al., 2015; Tzortziou et al., 2018). The relatively large footprint of OMI (~13x24 km^2 pixel resolution at nadir) and its coarse temporal resolution (1-2 overpasses per day) can further hinder good comparisons with ground-based NO_2 measurements. These issues also make it difficult for OMI to resolve land-water NO_2 pollution gradients (Tzortziou et al.,

2012; Tzortziou et al., 2015; Kollonige et al., 2018). In order to improve upon the issue of satellite pixel size, the European Space Agency (ESA) developed the Tropospheric Monitoring Instrument (TROPOMI), which was launched on the Sentinel-5 precursor satellite in late 2017. TROPOMI has a spatial resolution of ~3.7x7 km^2 for NO_2, which is nine times higher than that of OMI (Loyola et al., 2017; Griffin et al., 2019). The data became available in June of 2018, and they have the potential to yield better comparisons with PSI than are possible with OMI.

During the 2017 Ozone Water-Land Environmental Transitions Study (OWLETS) campaign, we compared total column NO_2 measurements from OMI and PSI. This campaign was focused on measurements at two sites: the inland NASA Langley Research Center (LaRC) site and the over-water Chesapeake Bay Bridge Tunnel (CBBT) site. CBBT was the less-polluted site, and average OMI-PSI agreement was ~15%. In contrast, average OMI-PSI agreement was ~29% at the more-polluted LaRC site. These results illustrate PSI's ability to detect statistically significant land-water gradients in NO_2 pollution. In addition, the OMI-PSI agreement was found to be the most compromised when OMI's pixel size coincident with the site exceeded ~13x24 km^2. This confirms that OMI's course spatial resolution is often an issue when making these comparisons.

In this study, we analyze results from satellite-PSI NO_2 comparisons using data from OMI and TROPOMI. The measurements were collected during and after the 2018 OWLETS-2 campaign in the Baltimore/Washington region. The main goals of this study were to: (1) Evaluate NO_2 measurements from satellites and PSI in a more polluted region along the Chesapeake Bay than tidewater Virginia, (2) Determine whether TROPOMI's higher resolution improves satellite-PSI comparisons as well as the capability of satellites to detect localized

pollution sources and gradients, (3) Evaluate conditions for which satellite-PSI discrepancies are greatest, and (4) Confirm PSI's ability to provide accurate, continuous air quality measurements.

Chapter 2. Methodology

2.1 OWLETS-2 Sites

As shown in in Figure 1, this study was centered around three sites: the University of Maryland, Baltimore County (UMBC), NASA's Goddard Space Flight Center (GSFC), and Hart Miller Island (HMI). Each site was affected by NO_2 pollution from a variety of sources, including mobile (i.e., automobiles and other vehicles), shipping emissions along the Chesapeake Bay, and power plants. UMBC (39.2547N, 76.7092W) is located about 25 km inland from the Chesapeake Bay and 7 km southwest of downtown Baltimore. The site is also located right between interstates 95 and 695, which means that it receives pollution from vehicle emissions as well as 8 power plants that are located nearby. The HMI site (39.2511N, 76.3666W) is located on the western side of Chesapeake Bay about 20 km east of downtown Baltimore. This site is subject to pollution from upwind urban and power plant emissions as well as shipping lanes. Due to Baltimore's proximity to the bay, the presence of bay-land breeze circulations can make for significant pollution gradients between UMBC and HMI. Lastly, the GSFC site (38.9896N, 76.8533W) is located about 38 km inland from the bay and 20 km northeast of downtown Washington, D.C. This site receives pollution mainly from local and upwind vehicle emissions. By examining all three sites, we are able to observe land-water NO_2 pollution gradients as well as gradients between the Baltimore and D.C. areas.

2.2 Satellite Column NO_2 Observations

2.2.1 Aura OMI

OMI is a UV-visible spectrometer that was first launched on NASA's Aura satellite in the summer of 2004. Measurements from OMI cover a spectral range of 264 to 500 nm, and the

nadir pixel size is about 13 by 24 km (Levelt et al., 2018). It passes above the equator daily between 1300 and 1400 UTC and achieves global coverage roughly every two days. As described previously, OMI uses direct and backscattered solar radiation to estimate total column amounts of NO_2 (Lamsal et al., 2017; Goldberg et al., 2017; Levelt et al., 2018). Due to the fact that the satellite scans are often at an angle relative to the local vertical, OMI actually calculates slanted NO_2 columns. These slant columns are then converted to vertical columns through algorithms using air mass factors, which are a function of cloud cover, aerosol concentrations, and basic meteorological parameters (Goldberg et al., 2017; Lamsal et al., 2017; Levelt et al., 2018). The OMI data used (Table 1) was level 2 (L2) un-gridded data and was obtained from NASA's GES DISC website: https://disc.gsfc.nasa.gov/datasets?page=1&source=AURA%20OMI. L2 refers to vertical column data that has not been changed (i.e. filtered or gridded). The data files also include variables such as cloud fractions and track quality flags, which are used to filter the data according to requirements. In order to ensure the quality of the data, OMI overpass pixels with cloud fraction values greater than 0.30 and/or quality control flags greater than 1 were excluded from the comparisons (Levelt et al., 2018).

2.2.2 Sentinel-5P TROPOMI

TROPOMI is a UV-visible spectrometer (like OMI) on ESA's Sentinel-5 Precursor satellite (Table 1) that measures solar backscatter and estimates total column NO_2 (Loyola et al., 2017; Griffin et al., 2019). The satellite was launched in late 2017 and passes over the equator once per day around 1300 UTC (~30 minutes earlier than OMI's overpasses). The instrument has a nadir pixel resolution of about 3.7 km by 7 km for NO_2 (Loyola et al., 2017; Griffin et al., 2019). TROPOMI is able to collect measurements in the UV-visible (270–500 nm), near-infrared

(675–775 nm), and shortwave infrared (2305–2385 nm) spectral regions (Loyola et al., 2017; Loyola et al., 2018; Griffin et al., 2019). This means that it can provide accurate measurements of a wide range of pollutants, including NO_2, ozone (O_3), formaldehyde (HCHO), and Sulphur dioxide (SO_2). Unlike with OMI, the NO_2 data and certain quality control parameters (e.g. cloud fraction) come in separate files. For quality assurance, data values with cloud fractions greater than 0.30 and/or quality control flags greater than 1 were excluded from the comparisons (Loyola et al., 2018; Griffin et al., 2019).

2.3 PSI Column NO_2 Measurements

Ground-based total column NO_2 measurements were obtained from PSI spectrometer instruments placed at UMBC, GSFC, and HMI (Table 1). The instrument measures solar radiation from 284-500 nm and collects data roughly every two minutes. PSI has a spectral resolution of about 0.6 nm and has an absolute error of ~0.05 DU and a precision of ~0.01 DU when no clouds are present (Herman et al., 2009; Tzortziou et al., 2012). The data used was obtained from the Pandonia online archive (https://pandonia.net/data) and consists of level 3 (L3) data that have gone through post-processing and spectral fitting (Knepp et al., 2015; Kollonige et al., 2018). The files also include quality control parameters (e.g. uncertainty and normalized root mean squared error (RMS)), which are used to filter for clouds and retrieval errors. In this study, data points with uncertainty and/or RMS values greater than 0.05 DU (~1.3×10^{15} molecules/cm^2) were discarded in order to minimize retrieval errors and cloud effects (Tzortziou et al., 2015; Kollonige et al., 2018).

2.4 Ancillary Data

2.4.1 Surface (In-Situ) NO_2 Measurements

In order to determine how well the satellites and PSI monitored trends in surface NO_2 pollution, we examined time series of in-situ NO_2 data collected during OWLETS-2 at each site. In-situ trace gas data were collected at HMI by the Maryland Department of the Environment (MDE), and data were collected at UMBC by scientists from both UMBC and NASA GSFC. Surface data at GSFC were collected by the Nittany Atmospheric Trailer and Integrated Validation Experiment (NATIVE), which is a mobile atmospheric research trailer that contains analyzers to measure O_3, CO, and NO_2 (Martins et al., 2012; Stauffer et al., 2015; Reed et al., 2015).

2.4.2 UMD Cessna 402B Aircraft NO_2 Measurements

NO_2 data collected by UMD's 402B Cessna aircraft was employed for viewing vertical profiles of pollution on selected days. This aircraft collected trace gas measurements between 0 and 5 km during OWLETS-2. For this study, aircraft NO_2 measurements were analyzed within a boxed domain (39.22-39.28N, 76.15-76.90W) that included HMI and UMBC. More information on the aircraft and missions can be obtained at: https://aosc.umd.edu/~flaggmd/?page_id=4.

2.4.3 LUFFT 15k Ceilometer and Ozonesondes

Measurements from a Lufft 15k ceilometer were used for PBL/mixing layer height estimations. This instrument uses a stable wavelength, narrow-line-width microchip laser operating at 1064 nm to measure aerosol backscatter between 0 and 15 km. It can also be used to estimate cloud and aerosol layers (Delgado et al., 2018). Mixing layer heights, residual layer heights, and cloud base heights were calculated externally using an algorithm developed by Dr.

Vanessa Caicedo at UMBC (Caicedo et al., 2017). For validation, PBL heights were also estimated using temperature profiles generated from ozonesondes launched at UMBC.

2.4.4 ERA-Interim Reanalysis Data

ERA-Interim reanalysis data was utilized for meteorological surface analyses during case studies performed on 29 June and 30 June 2018. This allowed for us to examine the influences of large-scale meteorology on the distribution of NO_2 pollution. We used mean sea-level pressure (MSLP) and 10 meter wind data for our analyses, and the data was obtained from the ERA-Interim website: https://www.ecmwf.int/en/forecasts/datasets/reanalysis-datasets/era-interim

2.5 Satellite-PSI NO_2 Comparisons

We compared PSI measurements to NO_2 retrievals from both OMI and TROPOMI. For OMI, singular points were created by averaging all overpass points within 25 km of the chosen site at a given time. For TROPOMI, all points within 3 km of the site were averaged due to the instrument's higher resolution. PSI column NO_2 measurements +/- 30 minutes on either side of the OMI and TROPOMI overpasses were averaged when the instruments were co-located in order to create a single value to use for each comparison. These comparisons only included satellite and PSI data that were not affected by clouds and/or retrieval errors. The agreement between satellite and PSI is given as percent differences calculated using the formula: [|x1-x2| / 0.5*(x1+x2)]*100%. These percent differences were binned into intervals of 10% to produce histograms of the satellite-PSI agreement at each site. This analysis is similar to those performed in Reed et al. (2015), Tzortziou et al. (2018), Kollonige et al. (2018), and Thompson et al. (2019).

Chapter 3. Results and Discussion

3.1 OMI-PSI Comparisons

When performing the OMI-PSI comparisons, the number of point comparisons at each site was limited due to the fact that most of the study days took place after the OWLETS-2 campaign (which ended on 7 July 2018). For example, the PSI instrument at HMI was not collecting data for extended periods of time after early July 2018. OMI overpasses were also limited due to cloud cover and retrieval errors. Thus, we only had 9 OMI-Pandora coincidences available for comparisons at UMBC; GSFC only had 16 values (Figure 2). The HMI site only had 5 points because clouds were more prevalent in the northern part of the OWLETS-2 region during July. Despite the limited number of points, the OMI-PSI comparisons at GSFC were consistent with results from previous studies. Specifically, the mean OMI-PSI percent difference for NO_2 was 19% at GSFC. In contrast, the mean percent difference at UMBC was 47%. This is far higher than the average offsets observed during OWLETS 2017. The explanation seems to be that the sites near Baltimore (UMBC and HMI) recorded more NO_2 pollution than GSFC, as detected by both satellites (Figure 2), PSI (Figure 2), and in-situ data (Figure 3). In addition, the OMI pixel sizes were rarely smaller than ~13x50 km^2 during this time period, suggesting that OMI's large footprint played a role in the disagreement at both sites. Both of these findings are consistent with the OWLETS 2017 results.

3.2 TROPOMI-PSI Comparisons

Whereas issues with clouds and retrieval errors are still present with the TROPOMI-PSI comparisons, less TROPOMI data had to be discarded. For UMBC, there were 25 satellite-Pandora coincidences that could be used for comparisons; GSFC had 28 values. As shown in

Figure 4, TROPOMI was more effective at capturing localized pollution plumes and gradients than OMI partly because of the smaller footprint, i.e. more nearly vertical coincidence with the measurement site. As a result, the satellite-PSI comparisons using TROPOMI were generally better at both sites than those performed with OMI (Figure 5). Specifically, the mean TROPOMI-PSI percent difference at GSFC is within 10% (9.4%), and the mean difference at UMBC is within 28%. These results show that the higher resolution of TROPOMI improves the agreement with PSI by roughly a factor of two. As with the OMI comparisons, the TROPOMI-PSI agreements are better at the less-polluted site(s). The overall improvement in the percent differences with TROPOMI is evident in Figure 6. In addition to better agreement, the higher resolution data from TROPOMI is far better correlated with PSI than OMI ($r = 0.82$ with TROPOMI versus $r = 0.18$ with OMI at GSFC), as displayed in Figure 7. The p-values from the t-tests are all less than 0.001, which demonstrates that there is statistical significance in the comparisons.

3.3 Case Studies

3.3.1 Case Study 1 (June 29, 2018)

June 29 was one of the few days during the campaign for which OMI-PSI agreement was superior to TROPOMI-PSI agreement. Specifically, TROPOMI-PSI agreement at UMBC was 28% at 17:12 UTC. OMI-PSI agreement at UMBC an hour and a half later (18:46 UTC) was 17%. In contrast, both OMI and TROPOMI agreed with PSI to within 5% at GSFC on this day. In order to explain these differences, we consider two factors: (1) vertical mixing and (2) OMI's pixel size and location. The OMI and TROPOMI UV-visible satellites are most sensitive to pollution that is located aloft. Thus, vertical mixing can distribute more NO_2 aloft and improve satellite-PSI comparisons. A surface pressure analysis at 1800 UTC shows that a weak high-

pressure system was centered to the West of the region (Figure 8). Weak northwesterly flow around this system transported urban NO_2 pollution southward from Baltimore, as shown in Figure 9. Ceilometer data at UMBC shows that the mixing layer grows by about 450 meters between the two satellite overpasses (Figure 10). The growth of the PBL and mixing layer throughout the afternoon is also evident on temperature soundings that were generated from ozonesonde data (Figure 11). Between the two overpasses, the aircraft data show NO_2 values aloft increasing by 1-1.2 ppb aloft (Figure 12), which indicates vertical redistribution of the pollution. On 29 June, OMI's resolution was close to the nadir value (~13x24 km^2) at the overpass, and a polluted pixel (~0.3 DU) was observed directly over UMBC (Figure 9). At this time, PSI measured 0.35 DU of NO_2 at UMBC, which is within 15% of what OMI measured. Earlier in the day, PSI also measured about 0.30 DU, but TROPOMI only measured ~0.2 DU at UMBC (Figure 9). Thus, it is likely that the redistribution of NO_2 pollution by vertical mixing as well as OMI's pixel location and resolution played a role in its superior agreement with PSI. The surface analyzers recorded higher NO_2 pollution on this day at UMBC (11 ppb at 17:12 UTC and 5.9 ppb at 18:46) than at GSFC (5.5 ppb at 17:12 UTC and 2.1 ppb at 18:46). In addition, PSI observed total column NO_2 values that were about 0.1 DU higher at UMBC than at GSFC.

3.3.2 Case Study 2 (June 30, 2018)

On the 30th of June, there was little NO_2 pollution at UMBC or GSFC (Figure 13). At 17:51 UTC, OMI-PSI agreement of 53% and 30% were observed at UMBC and GSFC, respectively. TROPOMI-PSI agreement was far better than OMI-PSI agreement on this day at UMBC (16% at 18:35 UTC) and GSFC (8.4% at 18:35 UTC). In addition, the TROPOMI-PSI agreement at both sites improved by roughly a factor of two from 16:53 UTC (35% at UMBC and 18% at GSFC). The surface pressure analysis at 1800 UTC indicates that the high-pressure system from the

previous day had strengthened and moved almost directly over the region (Figure 14). This is evident in the weak southwesterly flow over the region (Figure 14) and the strong subsidence inversion around 800 hPa at UMBC (Figure 15). The ceilometer profile at UMBC (Figure 16) shows that the mixing layer grows by about 300 meters between the two overpasses, which indicates that redistribution of NO_2 through vertical mixing likely improved the satellite-PSI comparisons. The ozonesonde temperature profiles also illustrate the growth of the PBL and mixing layer throughout the day (Figure 15). Besides the impact of mixing, OMI's poor agreement on 30 June can also be attributed to its pixel size, which was ~13x55 km^2 across the region. In addition, the surface values were 1-3 ppb higher at UMBC, and the PSI total column values were about 0.08-0.1 DU higher. Thus, the better satellite-PSI agreement was again observed at the cleaner site.

3.4 Discussion

The results from the OMI-PSI comparisons are consistent with what was observed during OWLETS 2017. The results showed that: (1) Cleaner, less-polluted sites show better satellite-PSI agreement than the more polluted sites and (2) The satellite-PSI comparisons suffer the most when OMI pixel size exceeds the nominal minimum, ~13x24 km^2. TROPOMI's higher resolution generally allowed for smaller offsets between satellite and PSI NO_2 measurements than are possible with OMI. Our analyses have shown that under cloud-free conditions, NO_2 measurements from the newer satellite and PSI can be expected to agree within 10% and display correlations greater than 0.50. This increases our confidence in satellite measurements of NO_2

pollution. The two case studies on 29 June and 30 June show examples of cleaner sites displaying better satellite-PSI agreement. Vertical mixing also plays an important role in the comparisons, and satellite-PSI comparisons can improve by a factor of two during the day as more NO_2 is mixed aloft.

Chapter 4. Summary and Conclusions

We compared total column NO_2 measurements from two satellite instruments (OMI and TROPOMI) with ground-based NO_2 column measurements from PSI in the mid-Atlantic region during summertime periods of varying pollution. In OWLETS 2017, we showed that OMI-PSI comparisons often suffer due to the coarse pixel resolution of OMI. However, TROPOMI's resolution is nine times higher than OMI, and the results show a significant improvement. In both the OWLETS and OWLETS-2 campaigns, the cleaner, less-polluted sites generally showed better satellite-PSI agreement. That being said, TROPOMI's higher resolution allows it to match up better with localized pollution sources measured by Pandora. This allowed for TROPOMI-PSI agreement to agree within 10% at the cleaner site (9.4% average at GSFC). The case studies were examined for 29 June and 30 June 2018 give some insights into how satellite-PSI agreement is better at the less-polluted sites. In addition, they show that OMI agrees better when the pixel size is smaller. The influence of vertical mixing on satellite-PSI agreement is illustrated by the fact that comparisons improve by a factor of two during the periods when the atmosphere becomes more well-mixed. Overall, the satellite-PSI agreement is improved by nearly a factor of two with TROPOMI at both sites, and much better correlations between satellite and PSI measurements are achieved ($r = 0.82$ with TROPOMI versus $r = 0.18$ with OMI at GSFC). In addition to showing that higher resolution satellite instruments can resolve localized NO_2 pollution, these results also demonstrate PSI's ability to provide accurate, continuous measurements of ground-based column NO_2 for air quality monitoring. Going forward, these results show that TROPOMI will be useful for detecting localized pollution in subsequent field campaigns.

References

Bucsela, E. J., Krotkov, N. A., Celarier, E. A., Lamsal, L. N., Swartz, W. H., Bhartia, P. K., … Pickering, K. E. (2013). A new stratospheric and tropospheric NO2 retrieval algorithm for nadir-viewing satellite instruments: Applications to OMI. Atmospheric Measurement Techniques, 6(10), 2607–2626. https://doi.org/10.5194/amt-6-2607-2013

Caicedo, V., Rappenglück, B., Lefer, B., Morris, G., Toledo, D., Delgado, R. (2017). Comparison of aerosol lidar retrieval methods for boundary layer height detection using ceilometer aerosol backscatter data, *Atmos. Meas. Tech.*, 10, 1609-1622, https://doi.org/10.5194/amt-10-1609-2017.

Delgado, R., Demoz, B., Sperling, M., Sasser, C., Alfa, E., Glover, M., et al. (2017). *OWLETS-2 UMBC Remote Sensing Capabilities and Air Quality Research*. *OWLETS Science Team Meeting*. Lecture presented at the OWLETS Science Team Meeting, Baltimore, MD: University of Maryland, Baltimore County.

Duncan, B. N., Lamsal, L. N., Thompson, A. M., Yoshida, Y., Lu, Z., Streets, D. G., … Pickering, K. E. (2016). A space-based, high-resolution view of notable changes in urban NOx pollution around the world (2005–2014). Journal of Geophysical Research: Atmospheres, 121, 976–996. https://doi.org/10.1002/2015JD024121

Flynn, C. M., Pickering, K. E., Crawford, J. H., Lamsal, L., Krotkov, N., Herman, J., … Brent, L. (2014). Relationship between column-density and surface mixing ratio: Statistical analysis of O3 and NO2 data from the July 2011 Maryland DISCOVER-AQ mission. Atmospheric Environment, 92, 429–441. https://doi.org/10.1016/j.atmosenv.2014.04.041

Goldberg, D. L., Lamsal, L. N., Loughner, C. P., Lu, Z., & Streets, D. G. (2017). A high-resolution and observationally constrained OMI NO_2 satellite retrieval. Atmospheric Chemistry and Physics Discussions, 1–26. doi:10.5194/acp-2017-219

Griffin, D., Zhao, X., McLinden, C. A., Boersma, F., Bourassa, A., Dammers, E., et al. (2019). High-resolution mapping of nitrogen dioxide with TROPOMI: First results and validation over the Canadian oil sands. *Geophysical Research Letters*, *46*. https://doi.org/10.1029/2018GL081095

Gurjar, B., Jain, A., Sharma, A., Agarwal, A., Gupta, P., Nagpure, A., & Lelieveld, J. (2010). Human health risks in megacities due to air pollution. Atmospheric Environment, 44(36), 4606–4613. doi:10.1016/j.atmosenv.2010.08.011

Herman, J., Cede, A., Spinei, E., Mount, G., Tzortziou, M., & Abuhassan, N. (2009). NO2 column amounts from ground-based PSI and MFDOAS spectrometers using the direct-Sun DOAS technique: Intercomparisons and application to OMI validation. Journal of Geophysical Research, 114, D13307. https://doi.org/10.1029/2009JD011848.

Herman, J., Spinei, E., Fried, A., Kim, J., Kim, J., Kim, W., et al. (2018). NO2 and HCHO measurements in Korea from 2012 to 2016 from PSI Spectrometer Instruments compared with OMI retrievals and with aircraft measurements during the KORUS-AQ campaign. *Atmospheric Measurement Techniques Discussions*, 1–60. doi:10.5194/amt-2018-56

Knepp, T., Pippin, M., Crawford, J., Chen, G., Szykman, J., Long, R., … Neil, D. (2015). Estimating surface NO2 and SO2 mixing ratios from fast-response total column observations and potential application to geostationary missions. Journal of Atmospheric Chemistry, 72(3-4), 261–286. https://doi.org/10.1007/s10874-013-9257-6

Kollonige, D. E., Thompson, A. M., Josipovic, M., Tzortziou, M., Beukes, J. P., Burger, R., Laakso, L. (2018). OMI satellite and ground-based PSI observations and their application to surface NO2estimations at terrestrial and marine sites. Journal of Geophysical Research: Atmospheres,123, 1441–1459.https://doi.org/10.1002/2017JD026518

Lamsal, L. N., Krotkov, N. A., Celarier, E. A., Swartz, W. H., Pickering, K. E., Bucsela, E. J., Gleason, J. F., Martin, R. V., Philip, S., Irie, H., Cede, A., Herman, J., Weinheimer, A., Szykman, J. J., and Knepp, T. N. (2014). Evaluation of OMI operational standard NO2 column retrievals using in situ and surface-based NO2 observations. Atmos. Chem. Phys., 14, 11587–11609. https://doi.org/10.5194/acp-14-11587-2014, 2014.

Lamsal, L. N., Duncan, B. N., Yoshida, Y., Krotkov, N. A., Pickering, K. E., Streets, D. G., & Lu, Z. (2015). U. S. NO2 trends (2005–2013): EPA air quality system (AQS) data versus improved observations from the ozone monitoring instrument (OMI). Atmospheric Environment, 110, 130–143. https://doi.org/10.1016/j.atmosenv.2015.03.055

Lamsal, L. N., S. J. Janz, N. A. Krotkov,K. E. Pickering, R. J. D. Spurr,M. G. Kowalewski, C. P. Loughner,J. H. Crawford, W. H. Swartz, andJ. R. Herman (2017), High-resolution NO2 observations from the Airborne Compact Atmospheric Mapper: Retrieval and validation, J. Geophys. Res.Atmos.,122, 1953–1970, doi:10.1002/2016JD025483

Lamsal, L. N., Martin, R. V., van Donkelaar, A., Steinbacher, M., Celarier, E. A., Bucsela, E., ... Pinto, J. P. (2008). Ground-level nitrogen dioxide concentrations inferred from the satellite-borne ozone monitoring instrument. Journal of Geophysical Research, 113, D16308. https://doi.org/10.1029/2007JD009235

Levelt, P. F., Joiner, J., Tamminen, J., Veefkind, J. P., Bhartia, P. K., Zweers, D. C., et al. (2018). The Ozone Monitoring Instrument: overview of 14 years in space. *Atmospheric Chemistry and Physics, 18*, 5699–5745. doi:https://doi.org/10.5194/acp-18-5699-2018

Loyola, D. G., García, S., Lutz, R., Romahn, F., Spurr, R. J. D., Pedergnana, M., … Schüssler, O. (2017). The operational cloud retrieval algorithms from TROPOMI on board Sentinel-5 precursor. Atmospheric Measurement Techniques Discussions, 1–30. https://doi.org/10.5194/amt-2017-128

Loyola, D., Veefkind, P., Aben, I., VanRoozendael, M., Siddans, R., Richter, A., & Wagner, T. (2018). Status of the operational Copernicus Sentinel-5 Precursor ... https://meetingorganizer.copernicus.org/EGU2018/EGU2018-19693.pdf. Accessed 31 March 2019

Lufft Ceilometer CHM 15k: A Passion for Precision. *Lufft Ceilometer CHM 15k: A Passion for Precision*. Carpinteria, CA: Lufft USA, Inc. https://www.lufft.com/fileadmin/lufft.com/07_downloads/4_brochures/brochure-lufft-CHM__04_2016_en.pdf. Accessed 31 March 2019

Martins, D.K., Stauffer, R., Thompson, A.M., Pippin, M., Knepp, T.: Surface ozone at a coastal suburban site in 2009 and 2010: Relationships to chemical and meteorological processes. J. Geophys. Res. 117, D05306 (2012). doi:10.1029/2011JD016828

Martins, D. K., Najjar, R. G., Tzortziou, M., Abuhassan, N., Thompson, A. M., & Kollonige, D. E. (2016). Spatial and temporal variability of ground and satellite column measurements of NO2 and O3 over the Atlantic Ocean during the deposition of atmospheric nitrogen to coastal ecosystems experiment (DANCE). Journal of Geophysical Research, 121(23), 14,175–14,187. https://doi.org/10.1002/2016JD024998

Reed, A. J., Thompson, A. M., Kollonige, D. E., Martins, D. K., Tzortziou, M. A., Herman, J. R., … Cede, A. (2012). Effects of local meteorology and aerosols on ozone and nitrogen dioxide retrievals from OMI and PSI spectrometers in Maryland, USA during DISCOVER-AQ 2011. Journal of Atmospheric Chemistry, 72(3-4), 455–482. https://doi.org/10.1007/s10874-013-9254-9

Sentinel-5P TROPOMI. (2018). *European Space Agency*. https://www.esa.int/Our_Activities/Observing_the_Earth/Copernicus/Sentinel-5P/Tropomi. Accessed 31 March 2019

Stauffer, R. M., Thompson, A.M., Martins, D.K., Clark, R.D., Goldberg, D.L., Loughner, C.P., Delgado, R., Dickerson, R.R., Stehr, J.W., Tzortziou, M.A.: Bay breeze influence on surface ozone at Edgewood, MD during July 2011. J. Atmos. Chem (2012). doi:10.1007/s10874-012-9241-6

Sullivan, J., T. Berkoff, G. Gronoff, T. Knepp, M. Pippin, D. Allen, L. Twigg, R. Swap, M. Tzortziou, A. Thompson, R. Stauffer, G. Wolfe, J. Flynn, S. Pusede, L. Judd, W. Moore, B. Baker, J. Al-Saadi, and T. McGee, 2018: The Ozone Water-Land Environmental Transition Study (OWLETS): An Innovative Strategy for AMERICAN METEOROLOGICAL SOCIETY Understanding Chesapeake Bay Pollution Events. Bull. Amer. Meteor. Soc. doi:10.1175/BAMS-D-18-0025.1, in press.

Thompson, A. M., Stauffer, R. M., Boyle, T. P., Kollonige, D. E., Miyazaki, K., Tzortziou, M., Herman, J. R., Jordan, C. E., Lamb, B. T. (2019). Comparison of near-surface NO_2 pollution with Pandora total column NO_2 during the Korea-United States Ocean Color (KORUS OC) campaign. Journal of Geophysical Research – Atmospheres. doi: 2019JD030765

Tzortziou, M., Herman, J. R., Cede, A., & Abuhassan, N. (2012). High precision, absolute total column ozone measurements from the PSI spectrometer system: Comparisons with data from a brewer double monochromator and Aura OMI. Journal of Geophysical Research, 117(D16), D16303. https://doi.org/10.1029/2012JD017814

Tzortziou, M., Herman, J. R., Loughner, C. P., Cede, A., Abuhassan, N., & Naik, S. (2015). Spatial and temporal variability of ozone and nitrogen dioxide over a major urban estuarine ecosystem. Journal of Atmospheric Chemistry, 72(3-4), 287–309. https://doi.org/10.1007/s10874-013-9255-8

Tzortziou, M., Parker, O., Lamb, B., Herman, J., Lamsal, L., Stauffer, R., and Abuhassan, N. (2018). Atmospheric trace gas (NO2 and O3) variability in Korean coastal waters, 614 implications for remote sensing of coastal ocean color dynamics, Remote Sens., 2018, 10, 1587; doi:10.3390/rs10101587.

Yang, W., & Omaye, S. T. (2009). Air pollutants, oxidative stress and human health. Mutation Research/Genetic Toxicology and Environmental Mutagenesis, 674(1-2), 45–54. doi:10.1016/j.mrgentox.2008.10.005

Figures

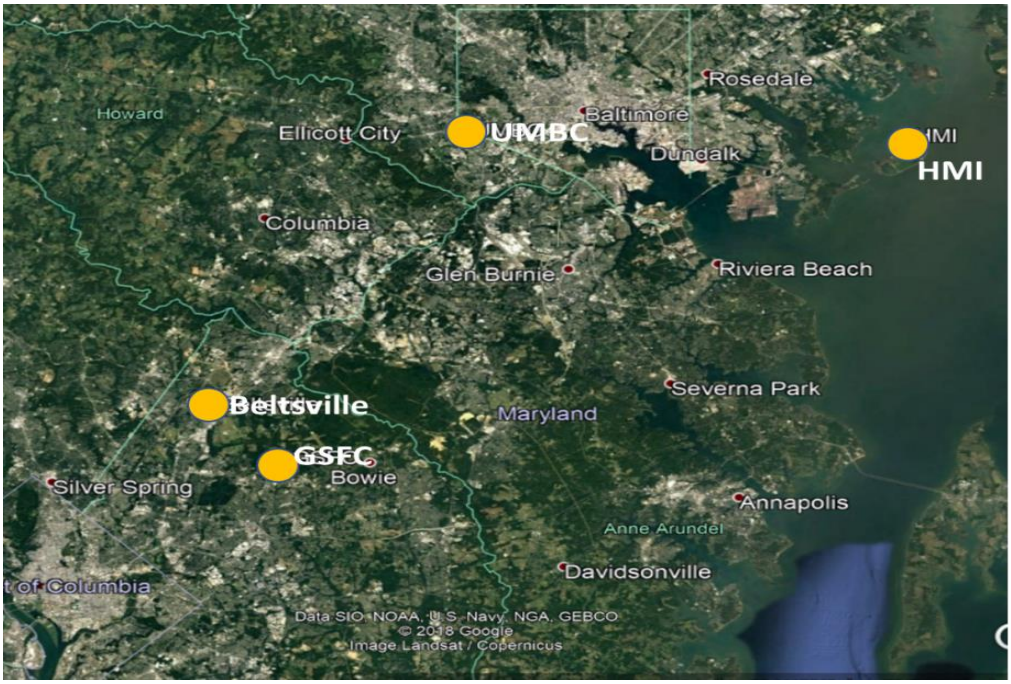

Figure 1: Geographic region and important sites for the OWLETS-2 campaign.

Instrument	Product(s)	Location(s)	Source
Pandora 19	Total Column NO_2	UMBC	Pandonia Online Archive: http://pandonia.net/data/
Pandora 30	Total Column NO_2	HMI	Pandonia Online Archive: http://pandonia.net/data/
Pandora 32	Total Column NO_2	GSFC	Pandonia Online Archive: http://pandonia.net/data/
Aura OMI	Total Column NO_2 and Cloud fraction	All sites	NASA DISC (Mirador) site: https://mirador.gsfc.nasa.gov/
Sentinel-5P TROPOMI	Total Column NO_2 and Cloud fraction	All sites	NASA GES DISC site: https://disc.gsfc.nasa.gov/datasets/
Surface NO_2 Monitors	In-situ surface NO_2	All Sites	OWLETS-2 Archive: https://www-air.larc.nasa.gov/cgi-bin/ArcView/owlets.2018
LUFFT 15k Ceilometer	Mixing Layer Height	UMBC	OWLETS-2 Archive: https://www-air.larc.nasa.gov/cgi-bin/ArcView/owlets.2018
UMD Cessna Aircraft	In-situ/flight-level NO_2	UMBC and HMI	OWLETS-2 Archive: https://www-air.larc.nasa.gov/cgi-bin/ArcView/owlets.2018
Ozonesondes	Vertical temperature and dew point profiles	UMBC	OWLETS-2 Archive: https://www-air.larc.nasa.gov/cgi-bin/ArcView/owlets.2018

Table 1: Summary of all instruments and data used in this study

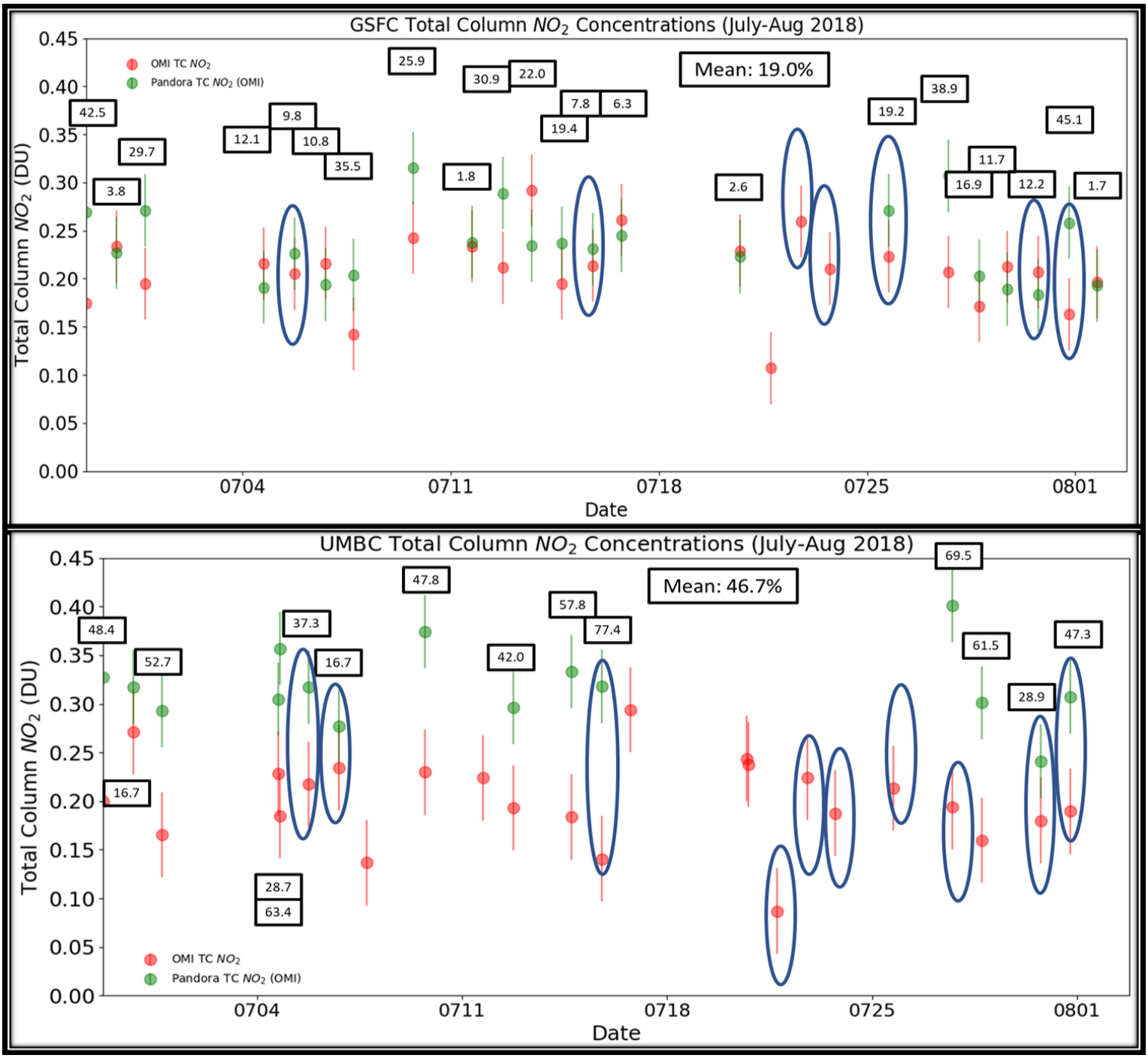

Figure 2: Comparison of TC NO_2 data from OMI and Pandora at GSFC (top) and UMBC (bottom). Ellipses represent "cloudy" days (cloud fraction >= 0.30), which were not used in the summary statistics.

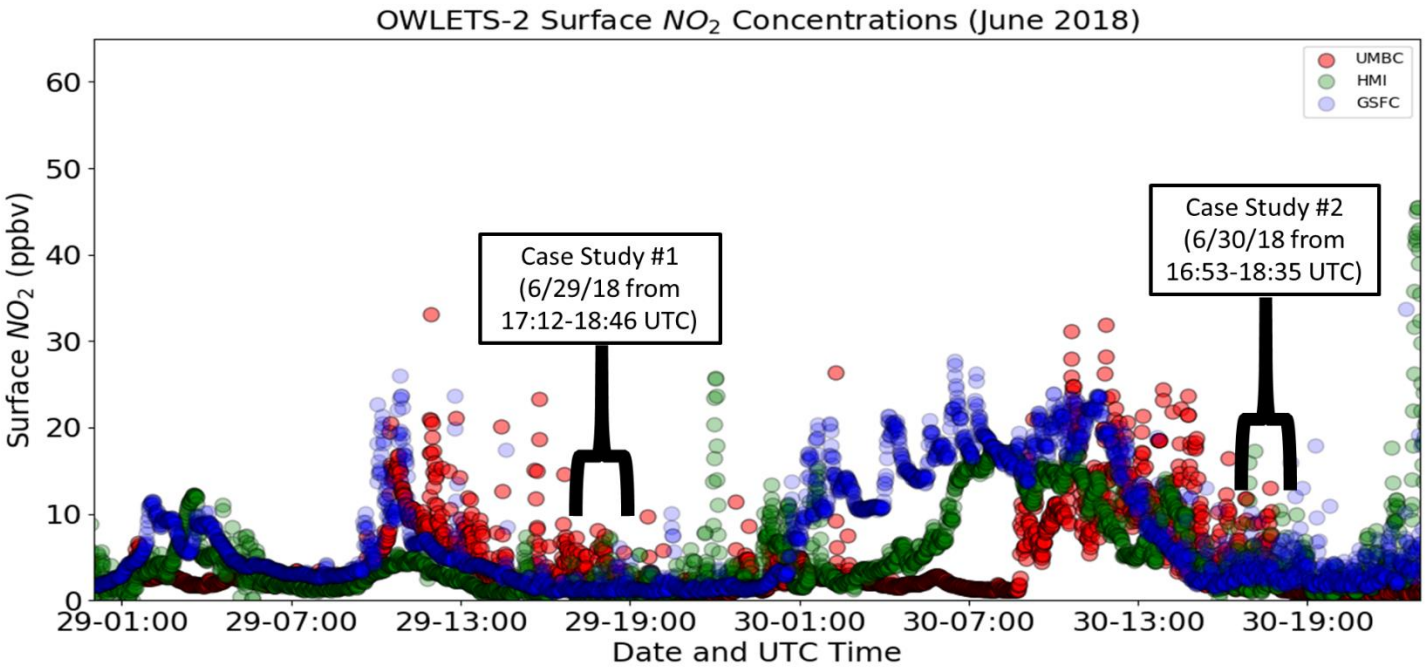

Figure 3: Time series of surface NO_2 concentrations at UMBC, HMI, and GSFC between 29 June and 30 June 2018. Black lines denote the time intervals of case studies to be presented later.

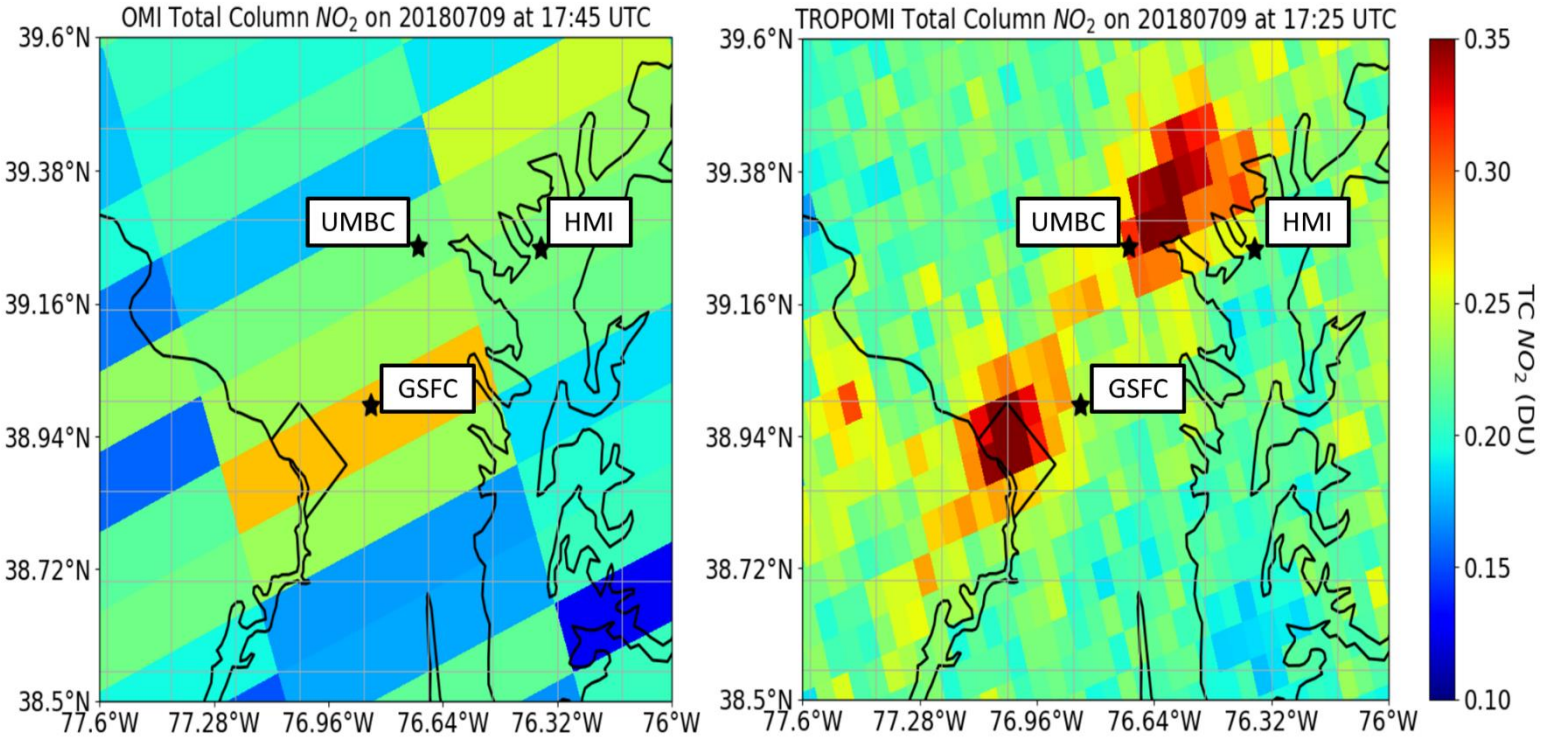

Figure 4: Comparison between OMI (left) and TROPOMI (right) TC NO_2 swaths on a polluted day (July 9, 2018)

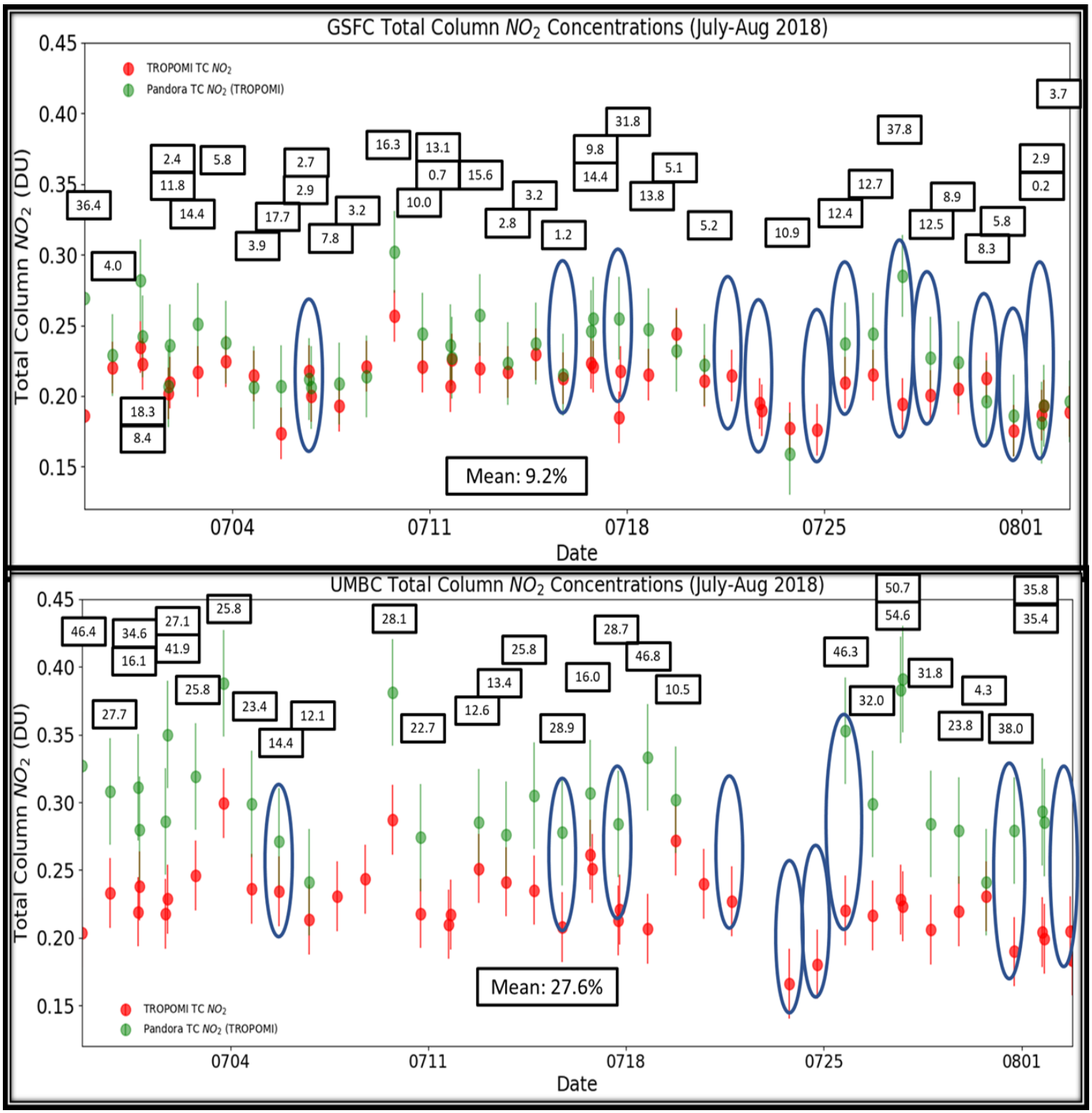

Figure 5: Comparison of TC NO_2 data from TROPOMI and Pandora at GSFC (top) and UMBC (bottom). Ellipses represent "cloudy" days (cloud fraction >= 0.30), which were not used in the summary statistics.

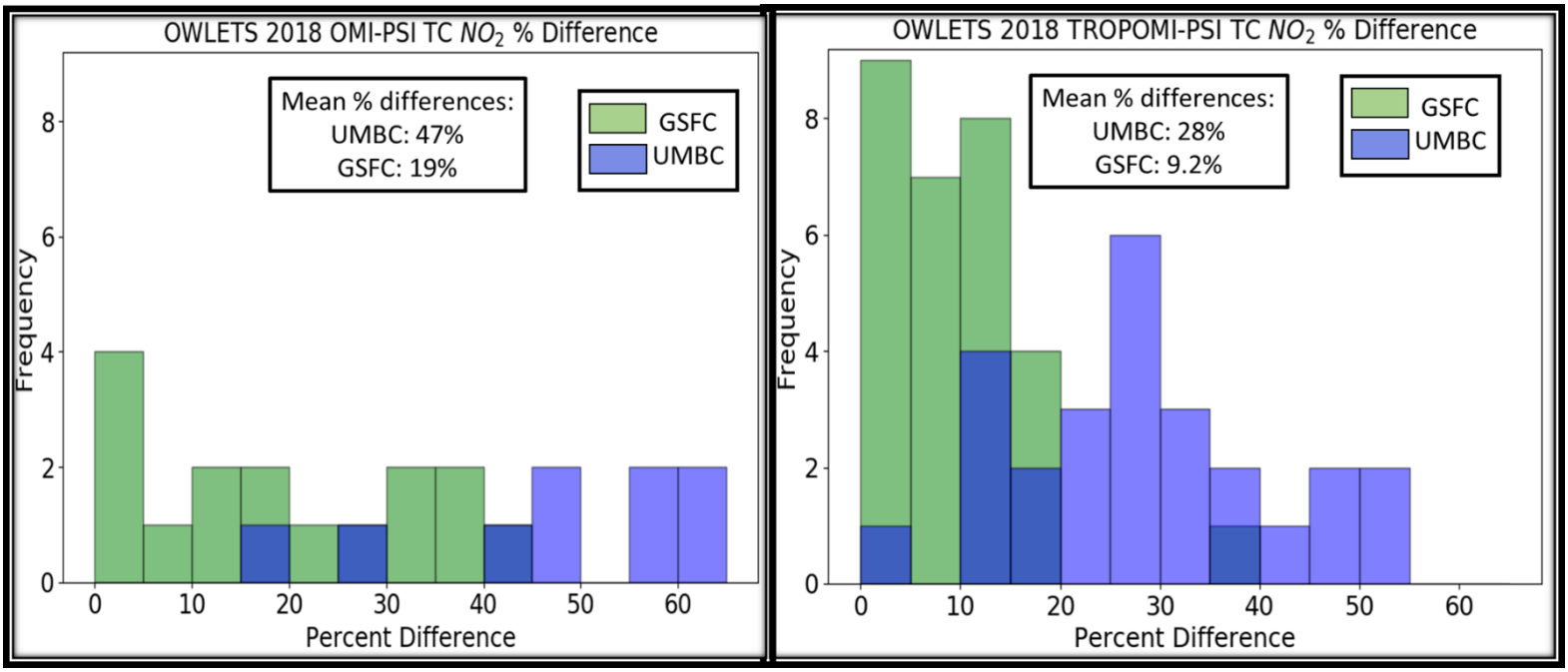

Figure 6: Histograms of OMI-Pandora (top) and TROPOMI-Pandora (bottom)TC NO_2 differences.

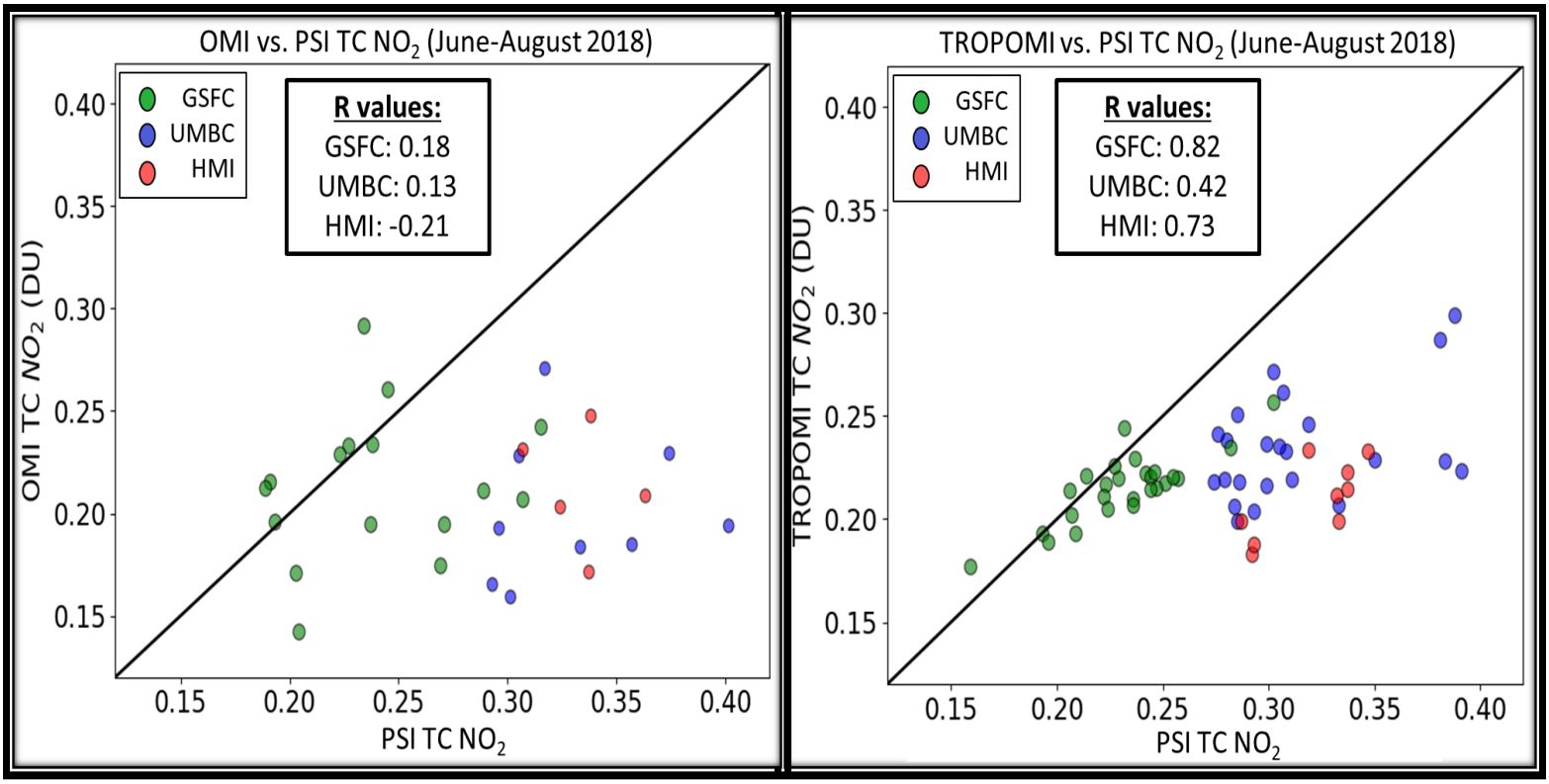

Figure 7: Comparison of Pandora TC NO_2 with OMI (left) and TROPOMI (right) retrievals at each site.

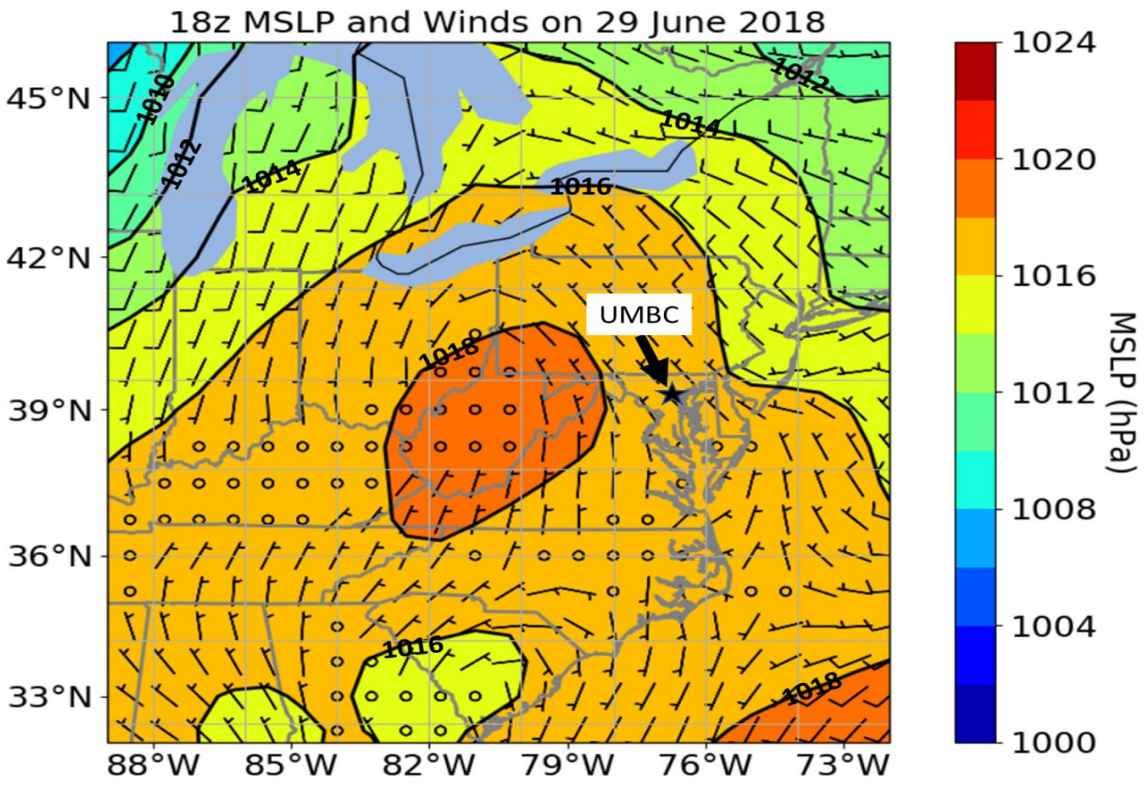

Figure 8: ERA-interim surface pressure and wind analysis at 18z on 29 June 2018

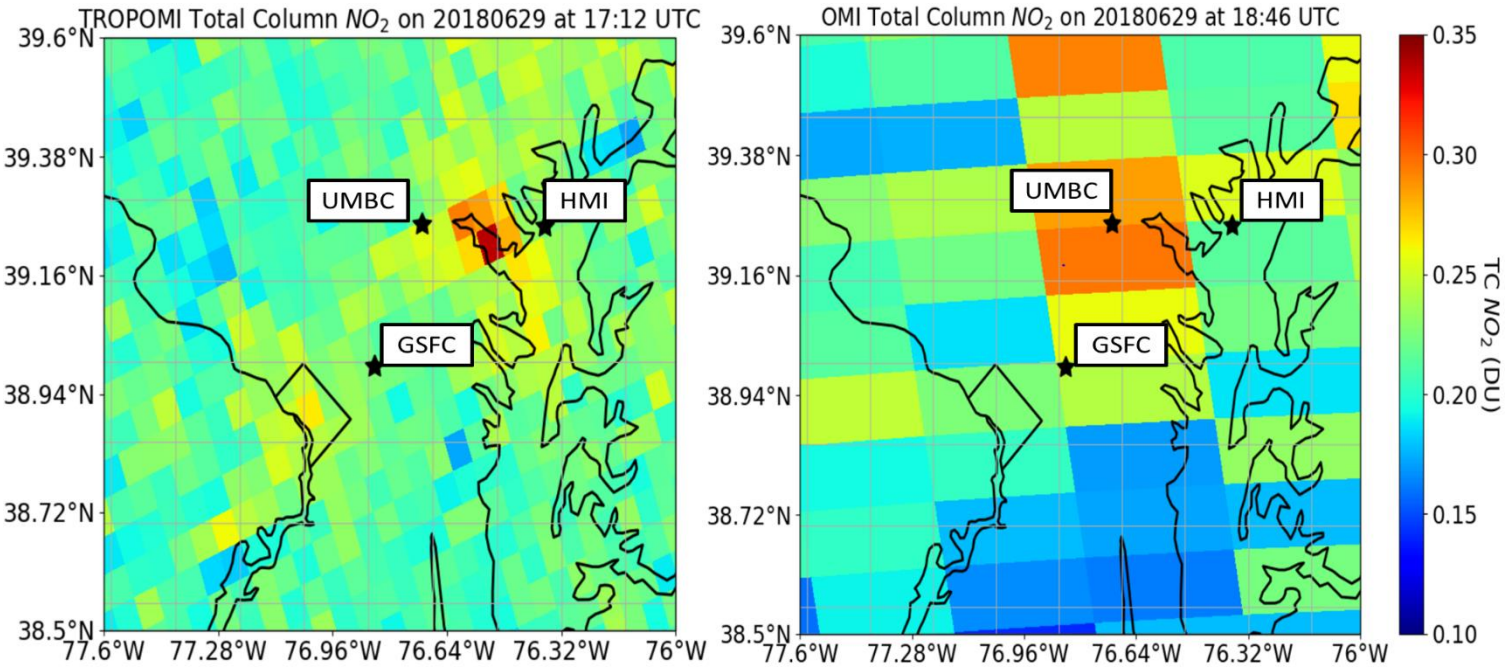

Figure 9: Comparison of TROPOMI (left) and OMI (right) total column NO_2 swaths on 6/29/18

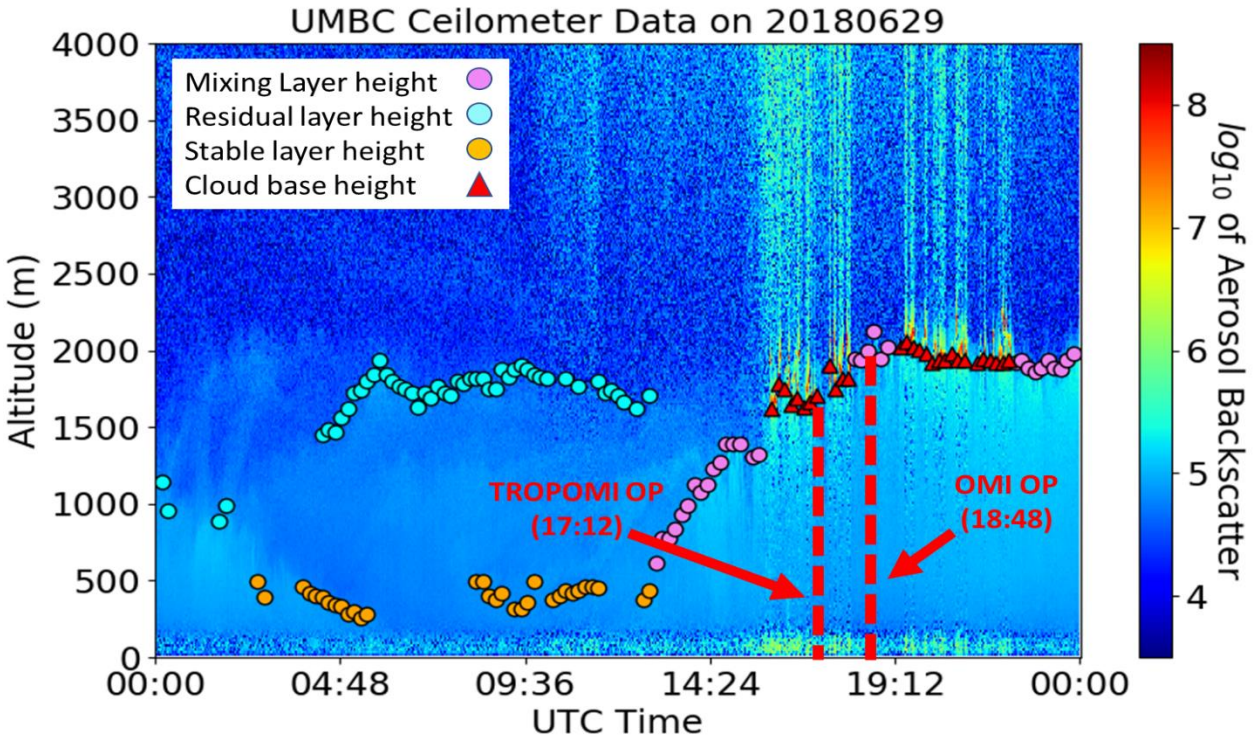

Figure 10: Aerosol backscatter curtain from the LUFFT 15k ceilometer at UMBC on 6/29/18. Red dotted lines indicate OMI/TROPOMI overpasses.

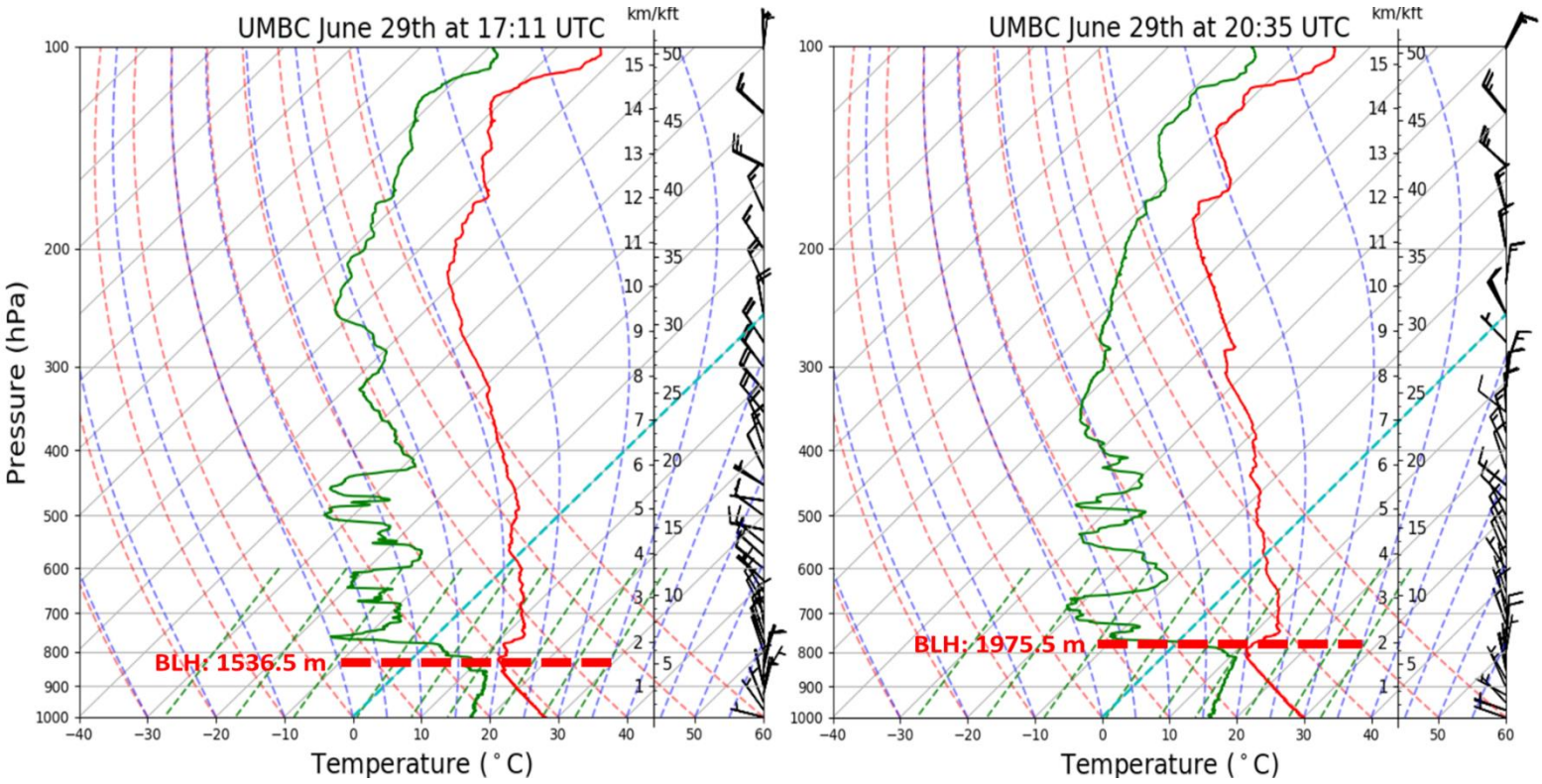

Figure 11: Skew-t/log-p diagrams generated from Ozonesonde data on 29 June 2018. Red dotted lines indicate PBL height estimates.

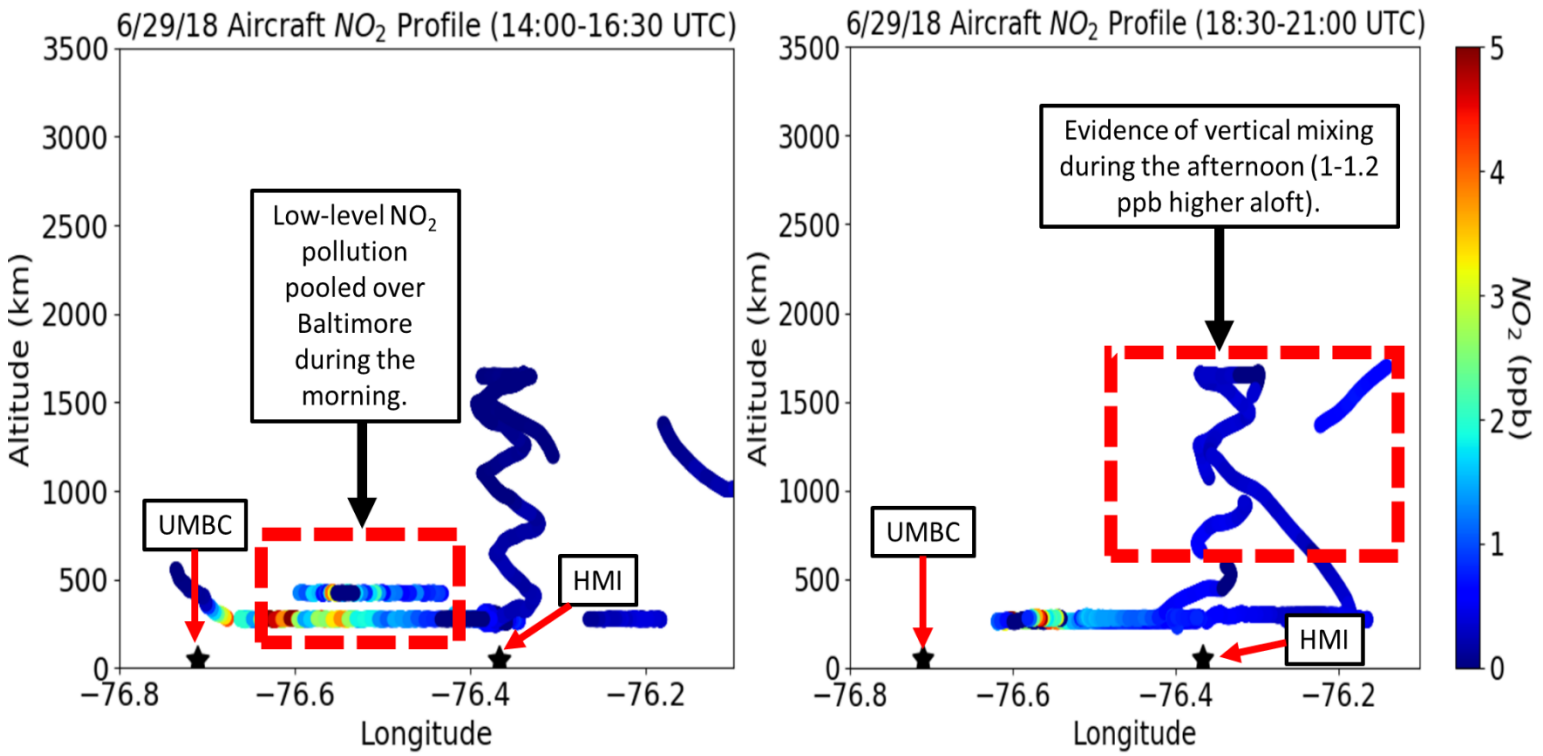

Figure 12: NO_2 profiles measured by the UMD Cessna Aircraft at 14:00 UTC and 18:30 UTC. Points shown are measurements collected between within domain spanning (25.22-25.28N) and (76-76.8W).

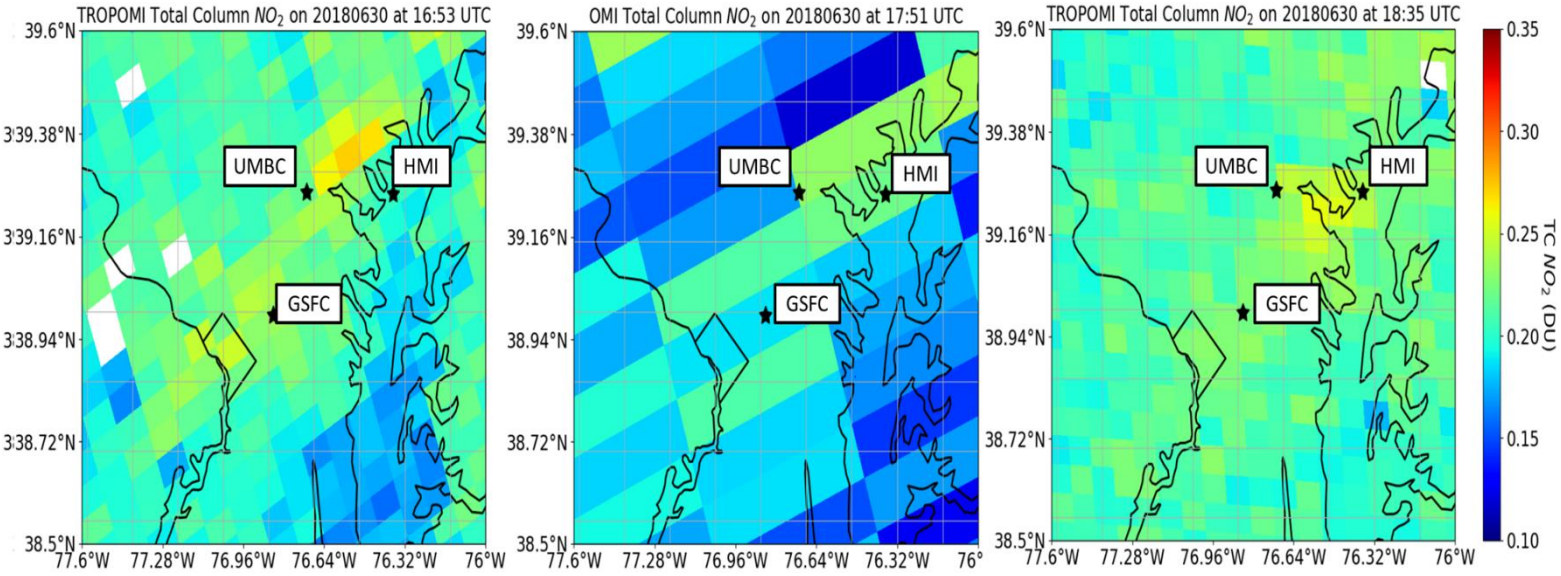

Figure 13: Comparison of TROPOMI (left and right) and OMI (middle) total column NO_2 swaths on 6/30/18

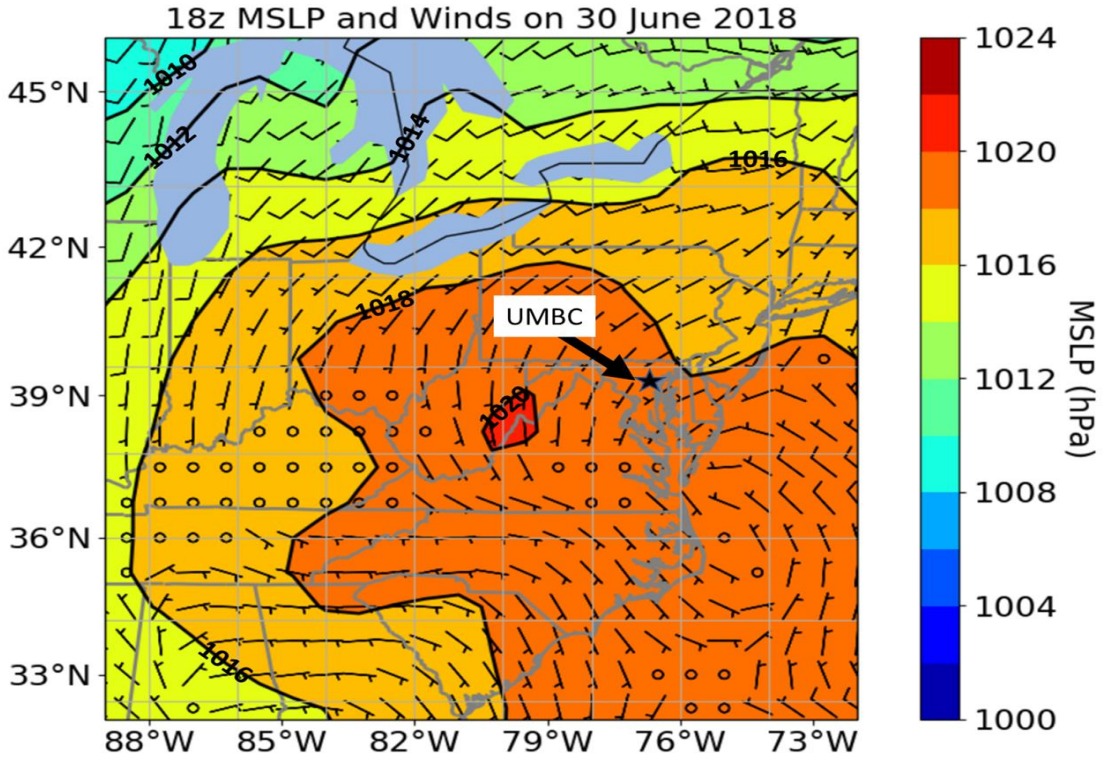

Figure 14: ERA-interim surface pressure and wind analysis at 18z on 30 June 2018

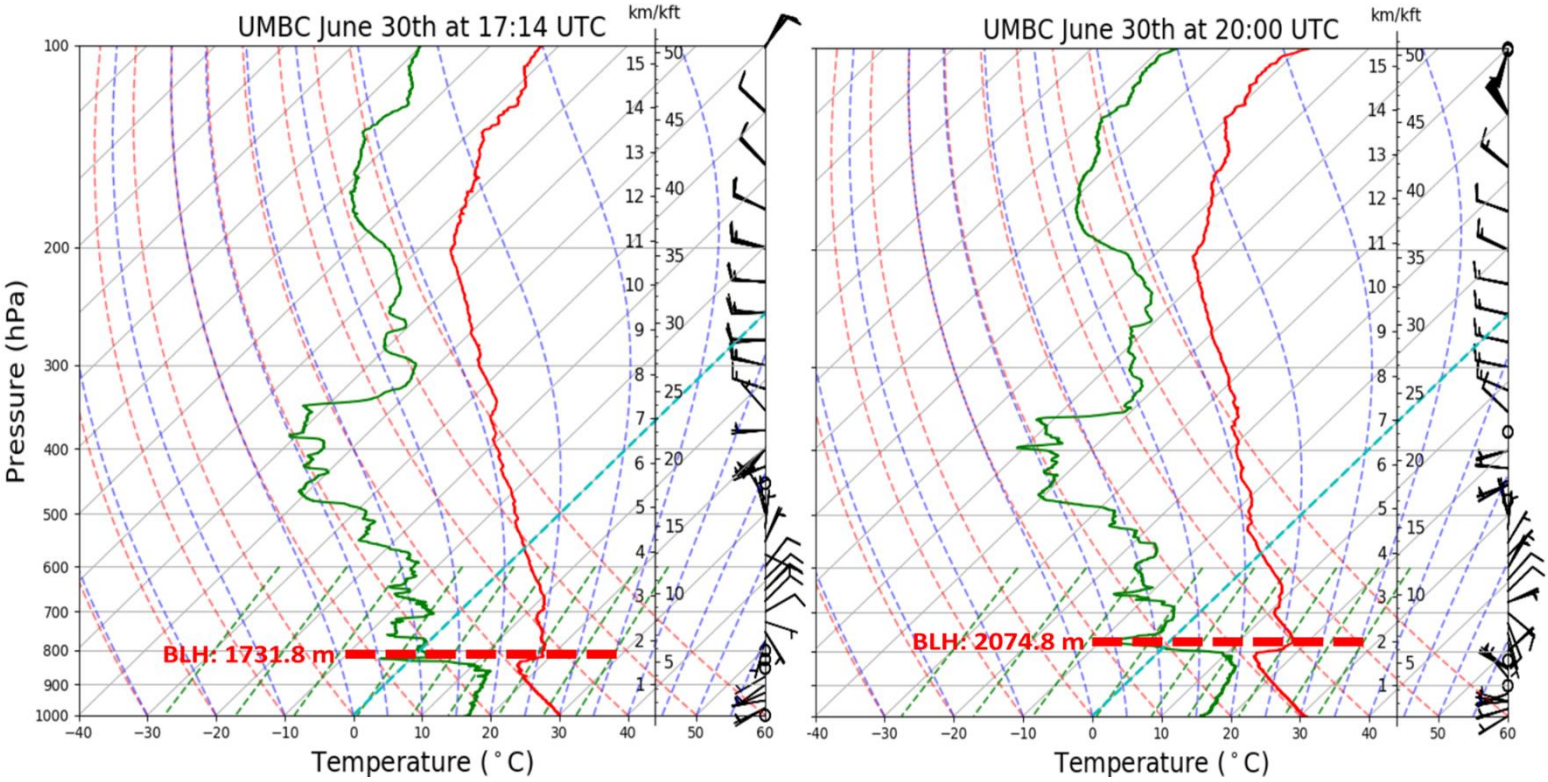

Figure 15: Skew-t/log-p diagrams generated from Ozonesonde data on 30 June 2018. Red dotted lines indicate PBL height estimates.

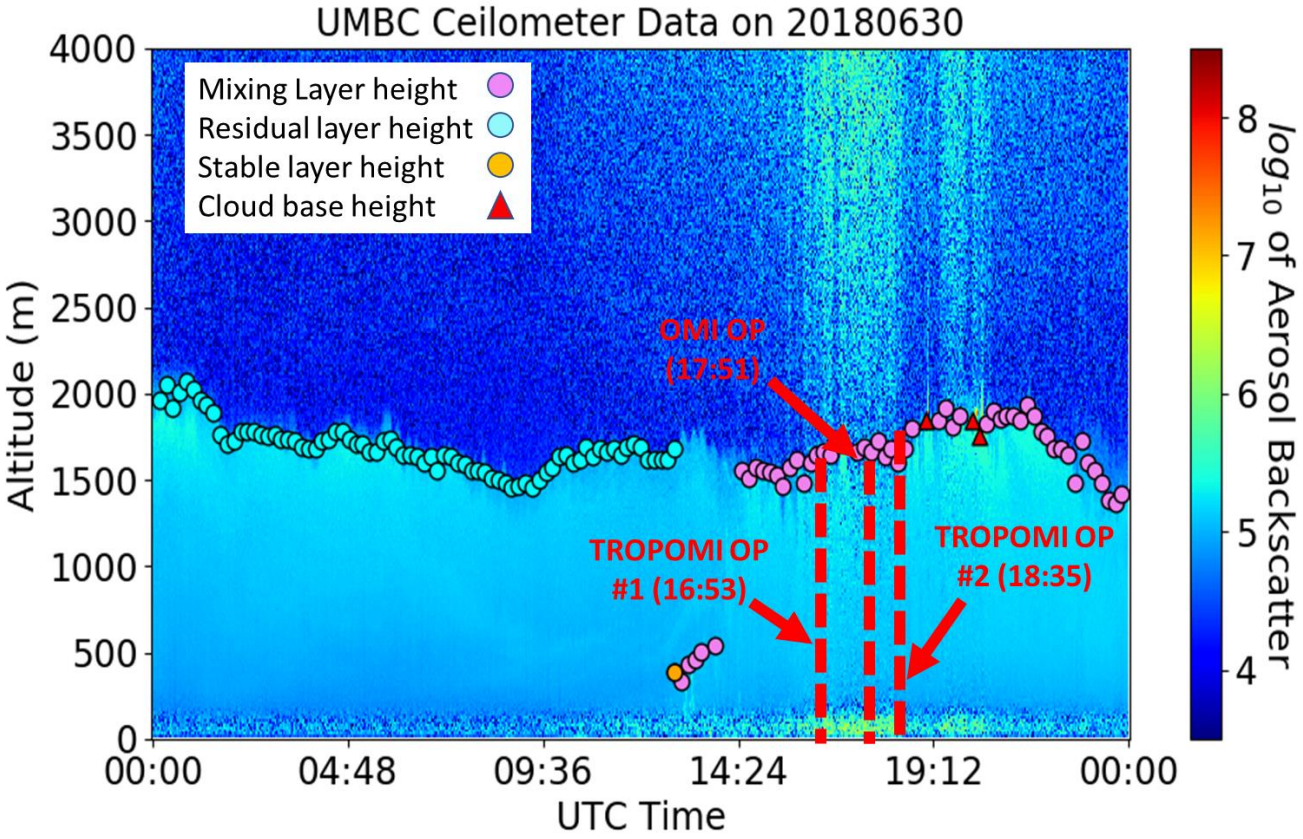

Figure 16: Aerosol backscatter curtain from the LUFFT 15k ceilometer at UMBC on 6/30/18. Red dotted lines indicate OMI/TROPOMI overpasses.

Supplementary Figures

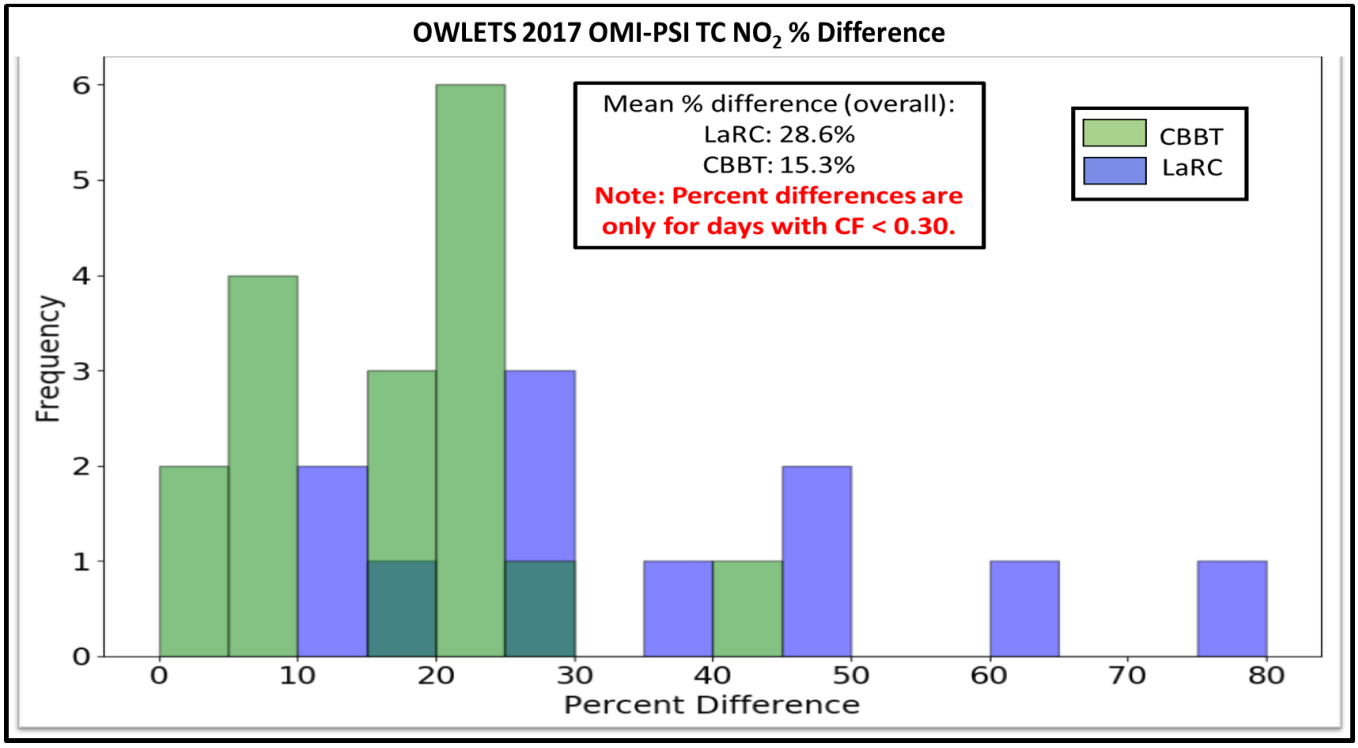

Figure 1S: Histogram of OMI-Pandora TC NO_2 percent differences at both OWLETS-1 sites

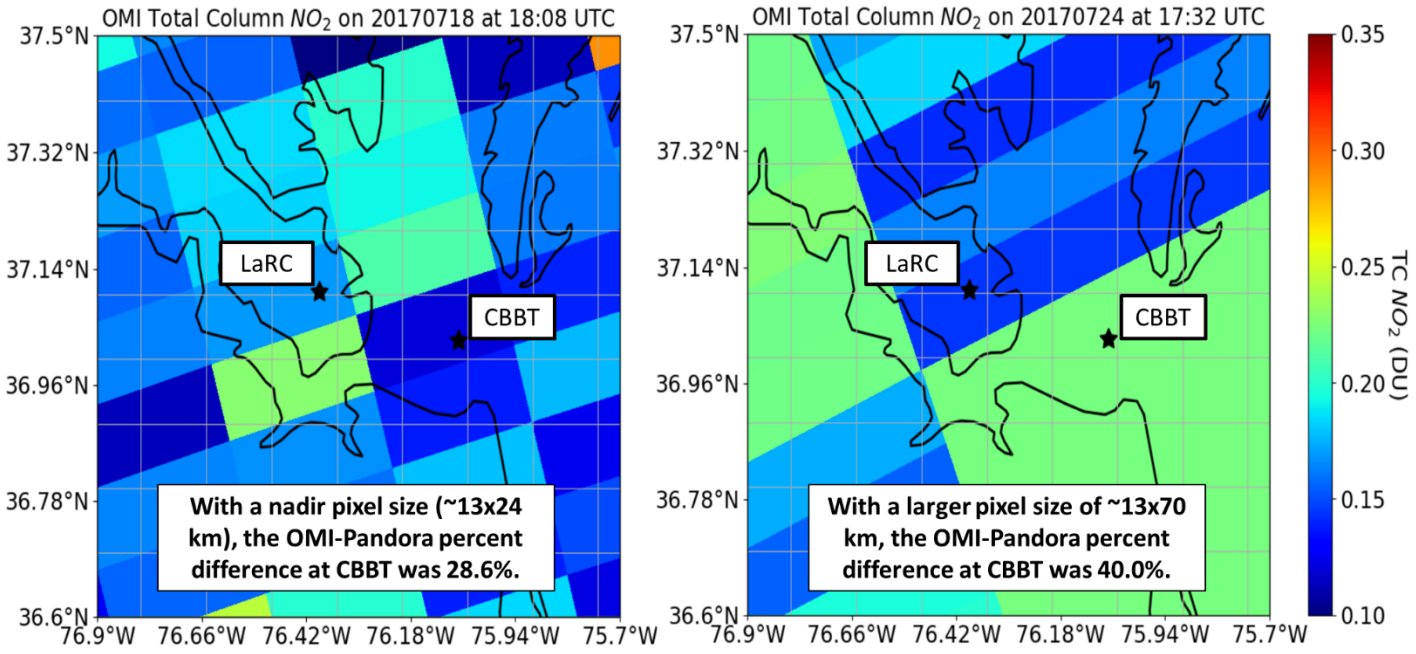

Figure 2S: Examples from OWLETS 2017 of "good" vs. "bad" pixel sizes for OMI total column NO_2 swaths

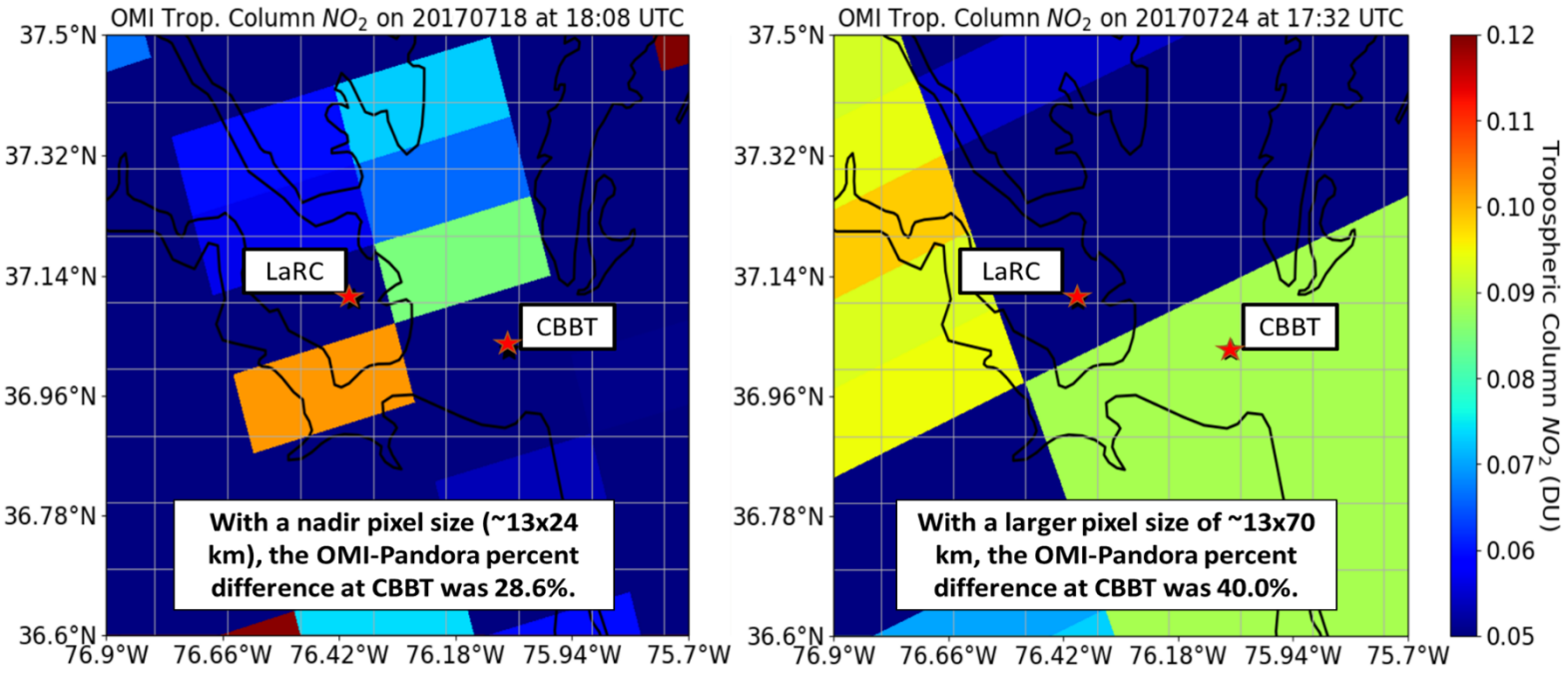

Figure 3S: Examples from OWLETS 2017 of "good" vs. "bad" pixel sizes for OMI tropospheric column NO_2 swaths

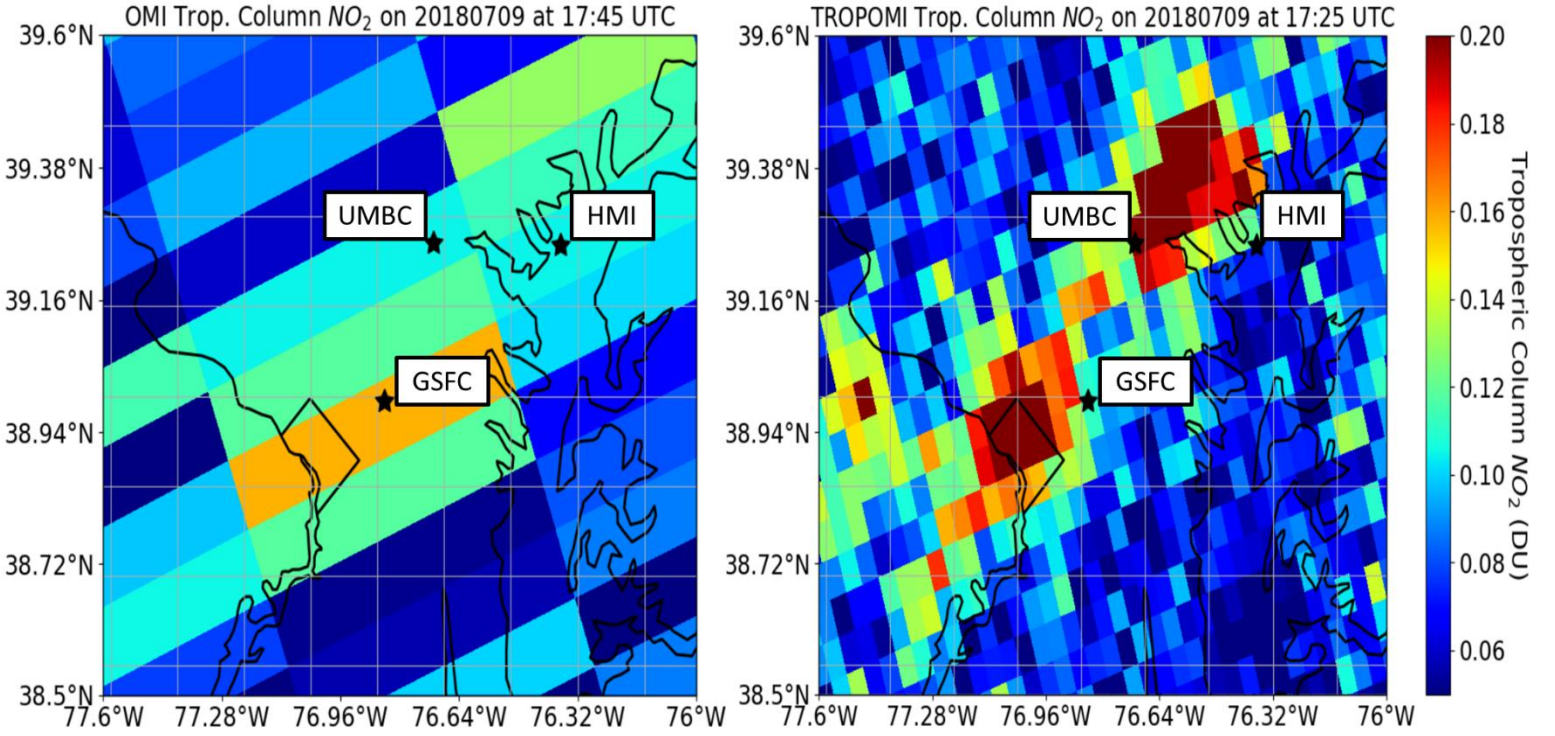

Figure 4S: Comparison between OMI (left) and TROPOMI (right) tropospheric column NO_2 swaths on a polluted day (July 9, 2018)

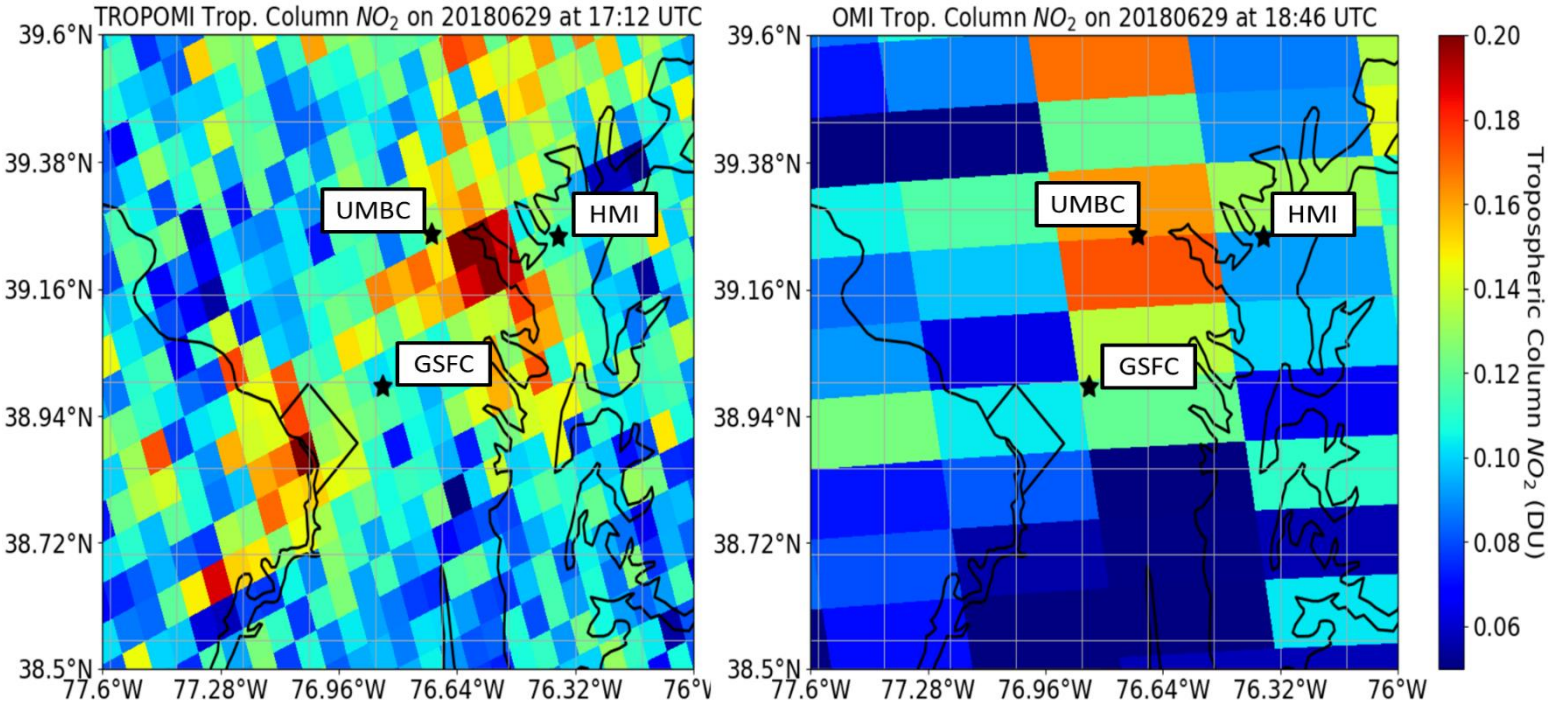

Figure 5S: Comparison of TROPOMI (left) and OMI (right) tropospheric column NO_2 swaths on 6/29/18

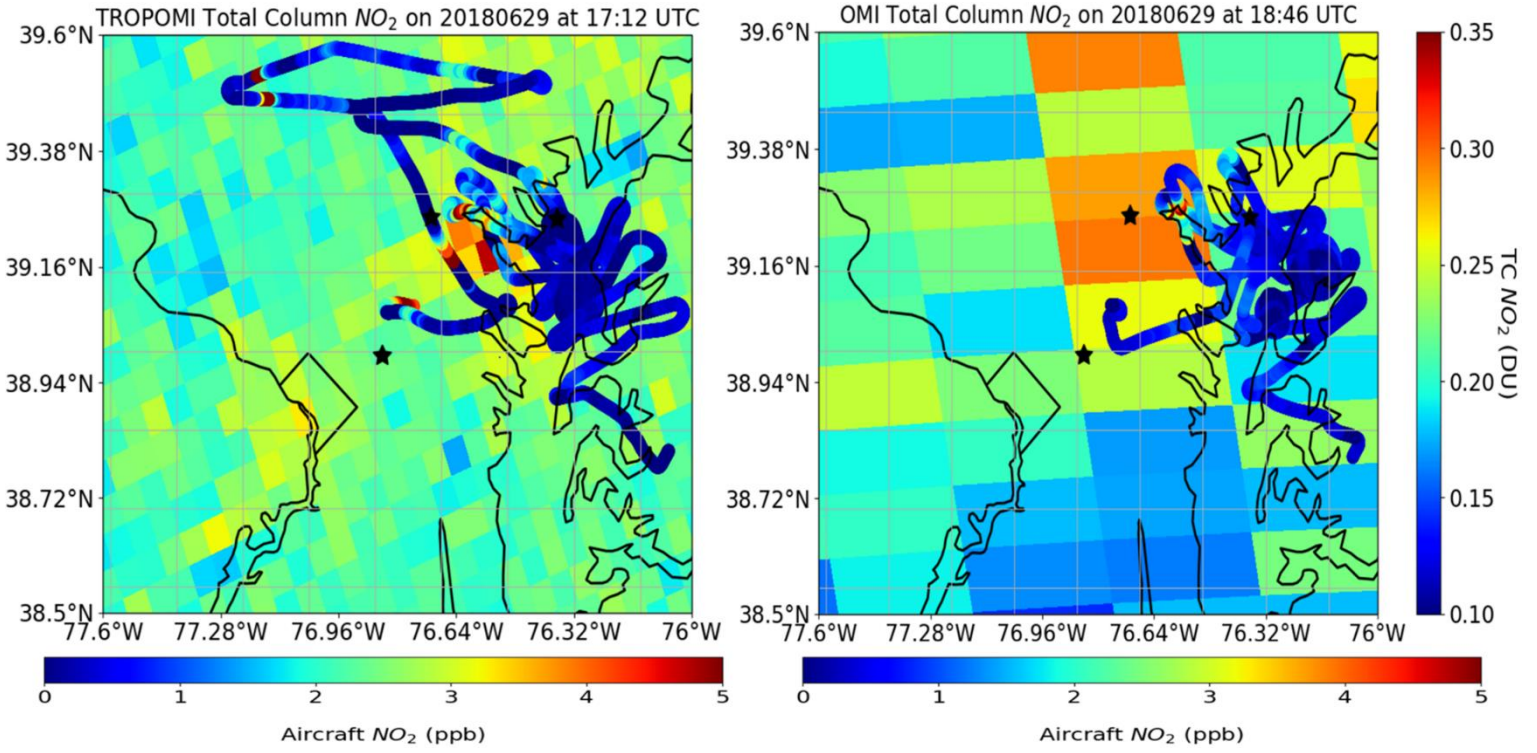

Figure 6S: UMD Cessna aircraft data overlaid on top of TROPOMI total column NO_2 swaths.

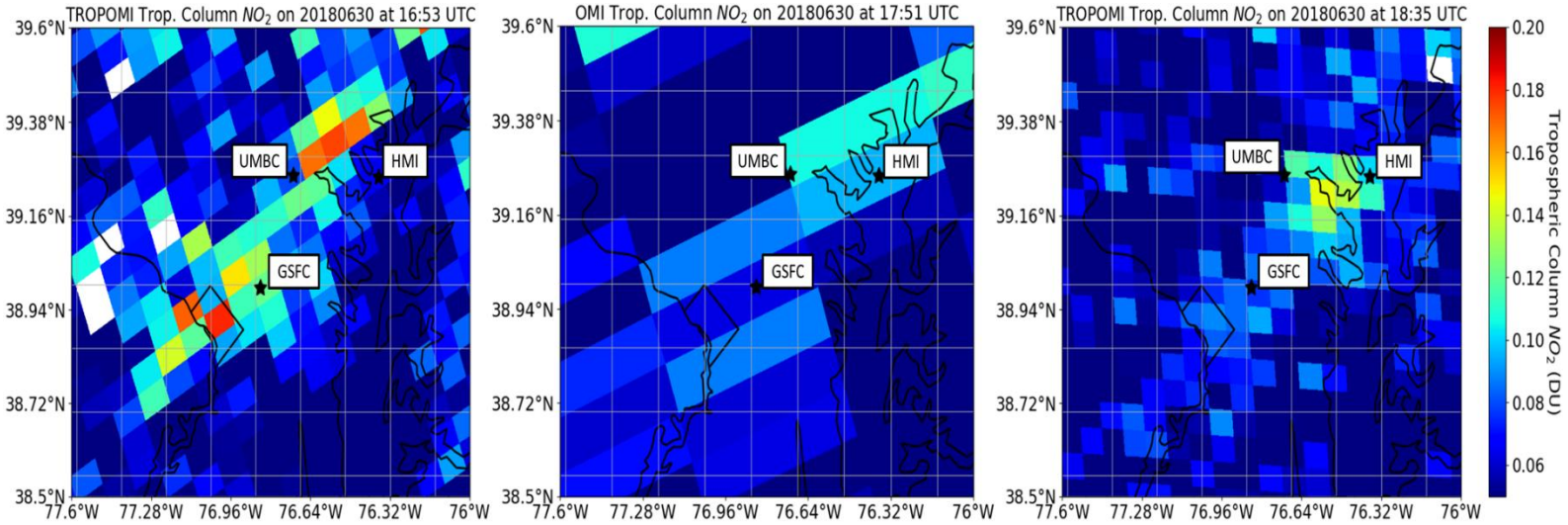

Figure 7S: Comparison of TROPOMI (left and right) and OMI (middle) tropospheric column NO_2 swaths on 6/30/18

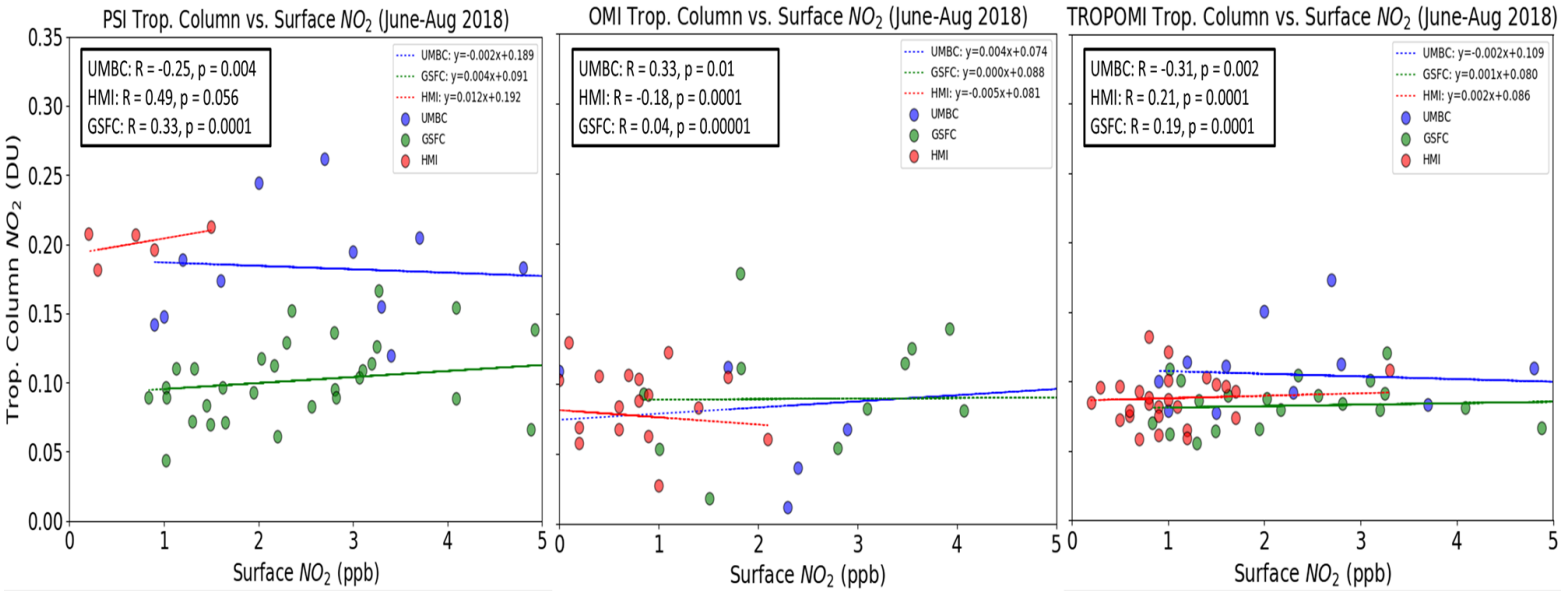

Figure 8S: Comparison of surface NO_2 values with tropospheric column NO_2 values from Pandora (left), OMI (middle), and TROPOMI (right). Lines represent linear fits between the surface and column values at each site.